HAMILTON STANDARD Division of United Technologies

CR 151982
SVHSER 7163

DESIGN, DEVELOPMENT, AND FABRICATION OF A PROTOTYPE ICE PACK HEAT SINK SUBSYSTEM

POTASSIUM BIFLUORIDE/WATER SOLUTION INVESTIGATIONS

FINAL REPORT

BY

GEORGE J. ROEBELEN, JR

AND

JORDAN D. KELLNER

PREPARED UNDER CONTRACT NO. NAS 2-8665

BY

HAMILTON STANDARD
DIVISION OF UNITED TECHNOLOGIES CORPORATION
WINDSOR LOCKS, CONNECTICUT 06096

FOR

NATIONAL AERONAUTICS AND SPACE ADMINISTRATION
AMES RESEARCH CENTER
MOFFETT FIELD, CALIFORNIA 94035

February 1977

HAMILTON STANDARD Division of UNITED TECHNOLOGIES

CR 151982
SVHSER 7163

DESIGN, DEVELOPMENT, AND FABRICATION OF A PROTOTYPE ICE PACK HEAT SINK SUBSYSTEM

POTASSIUM BIFLUORIDE/WATER SOLUTION INVESTIGATIONS

FINAL REPORT

BY

GEORGE J. ROEBELEN, JR

AND

JORDAN D. KELLNER

PREPARED UNDER CONTRACT NO. NAS 2-8665

BY

HAMILTON STANDARD
DIVISION OF UNITED TECHNOLOGIES CORPORATION
WINDSOR LOCKS, CONNECTICUT 06096

FOR

NATIONAL AERONAUTICS AND SPACE ADMINISTRATION
AMES RESEARCH CENTER
MOFFETT FIELD, CALIFORNIA 94035

February 1977

FOREWORD

This report has been prepared by Hamilton Standard, Division of United Technologies Corporation for the National Aeronantics and Space Administration, Ames Research Center in accordance with the requirements of Contract NAS 2-8665, Design, Development, and Fabrication of a Prototype Ice Pack Heat Sink Subsystem-Potassium Bifluoride/Water Solution Investigations.

Appreciation is expressed to the NASA Technical Managers, Mr. James Blackaby and Mr. Bruce Webbon of the Ames Research Center, for their guidance and advice.

Hamilton Standared personnel responsible for the conduct of this program were Mr. Daniel J. Lizdas, Program Manager, and George J. Roebelen, Jr, Project Engineering Manager. Appreciation is expressed to Mr. John S. Lovell, Chief, Advanced Engineering, and Mr. Edward H. Tepper, Senior Analytical Engineer, whose efforts made the successful completion of this program possible.

United Technologies Research Center personnel responsible for the potassium bifluoride/water properties measurements were Dr. Jordan D. Kellner, Principal Investigator, and Mr. David G. McMahon, Chief, Chemical Sciences.

TABLE OF CONTENTS

LIST OF FIGURES

LIST OF TABLES

INTRODUCTION

Future manned space exploration missions are expected to include requirements for astronaut life support equipment capable of repeated use and regeneration for many extravehicular activity (EVA) sorties. In anticipation of these requirements, NASA ARC funded two contracts (NAS 2-6021 and NAS 2-6022) for the study of Advanced Extravehicular Protective Systems (AEPS). The purpose of these studies was to determine the most practical and promising concepts for manned space flight operations projected for the late 1970's and 1980's, and to identify areas where concentrated research would be most effective in the development of these concepts.

One regenerative concept for astronaut cooling utilizes an ice pack as the primary heat sink for a liquid cooling garment (LCG) cooling system. NASA ARC funded a contract (NAS 2-7011) which resulted in:the design, fabrication, and test at one gravity of a prototype Ice Pack Heat Sink Subsystem; a study to uncover a material with a greater heat of fusion that could be substituted for water/ice as the thermal sink thereby reducing system weight and volume; and a plan for development of a candidate Shuttle/ Spacelab flight experiment capable of demonstrating the performance of an Ice Pack Heat Sink Subsystem for astronaut cooling in zero gravity as well as providing data on the physical phenomena associated preimarily with the heat transfer aspects of the operation of such a system. A concept for the Flight Experiment Physical Phenomena Experiment Chest was generated under a contract funded by NASA ARC (NAS 2-8665 Phase I).

This report describes the effort funded by NASA ARC under contract NAS 2-8665 Phase II during which time the potassium bifluoride/ water material selected under contract NAS 2-7011 was further developed as a viable thermal storage device.

SUMMARY

The objective of the Potassium Bifluoride/Water Solution Investigations was to further develop the concept of a potassium bifluoride/water solution as the heat sink material for a Regenerable Portable Life Support System.

Data have been generated to describe the properties of potassium bifluoride/water solution in the following areas:

Corrosion resistance of various materials with a potassium bifluoride/water solution.

Determination of the concentration of potassium bifluoride in water to obtain optimum heat absorption properties.

Heat absorption capability of potassium bifluoride/water solution contained in wick media.

Thermal conductivity of liquid and solid potassium bifluoride/water solutions.

Effect of long term cycling on potassium bifluoride/water heat absorption properties.

Volume change with temperature of liquid and solid potassium bifluoride/water solutions.

Effects of solution freeze rate and mechanical agitation on potassium bifluoride/water heat absorption properties.

Based on the results of this program, significant properties of the potassium bifluoride/water solution have been characterized and areas requiring further investigation have been identified.

CONCLUSIONS

As a result of the work completed during this program phase, the following conclusions were established concerning the potassium bifluoride/water solution:

1. Inconel 625, Hastelloy C, and AISI 347 have been demonstrated to be acceptable for use with potassium bifluoride/water solution. These materials are acceptable for use with each other in the solution due to their similar position in the electromotive force series.

2. The concentration of potassium bifluoride in water for optimum heat absorption has been experimentally determined to be 20% by weight.

3. Heat absorption capability of potassium bifluoride solutions is independent of the number of freeze/thaw cycles to which the solution is subjected.

4. Thermal conductivity of the liquid and solid bifluoride/water solution was experimentally determined to be 0.535 $W/m^{o}C$ and 2.31 $W/m^{o}C$, respectively.

5. Thermal expansion of the liquid potassium bifluoride/water solution was experimentally determined to be 1.74×10^{-4} $cm^3/cm^3\ ^{o}C$ from 3°C to 25°C and of the solid to be 1.02×10^{-4} $cm^3/cm^3\ ^{o}C$ from -14.8°C to -31.5°C. The volume change on freezing was determined to be 0.095 cm^3/cm^3.

6. Thermal conductivity of the liquid and solid potassium bifluoride/water solution when slurried with 10% by volume of ethanol was experimentally determined to be 0.454 $W/m^{o}C$ and 0.989 $W/m^{o}C$ respectively.

7. Thermal expansion of the potassium bifluoride/water solution when slurried with 10% by volume of ethanol was experimentally determined to be as described by Figure 12.

8. Mechanical agitation of the potassium bifluoride/water solution during thawing produces insignificant effect on heat absorption capability.

9. The rate of freeze of the potassium bifluoride/water solution significantly effects the heat absorption capability during subsequent melting. Testing performed to date and documented in the Large Sample Testing section is insufficient to allow a definitive conclusion regarding the magnitude of this effect.

10. The wicking testing has shown that the heat absorption capacity of potassium bifluoride in water when contained in a dacron felt wick media is severly decreased over that expected from unwicked calorimeter testing.

RECOMMENDATIONS

The studies and test results of this program have indicated that further definition of the characteristics of the potassium bifluoride/water solution is required. Both of the following tasks are recommended in order to fully characterize and evaluate the potassium bifluoride/water solution. If this is not feasible due to funding or other limitations, either task 1, which is fundamentally a scientific approach, or task 2, which is fundamentally an engineering approach, may be pursued independently.

Task 1: Generation of a liquid-solid phase diagram for the potassium bifluoride/water solution to aid in understanding the effect of freeze rate on the resulting chemical formations and, hence, the heat absorption capability of the material. This diagram is necessary to fully evaluate the potential of the solution for further applications.

Task 2: Additional modification and testing at controlled freezing rates utilizing the Paar adiabatic calorimeter to experimentally develop and verify heat absorption parameters associated with the freeze rate of the potassium bifluoride/water solution.

NOMENCLATURE

Btu	British thermal unit
cm	centimeter
°C	degrees Celsius
g	gram
hr	hour
HSD	Hamilton Standard Division
H/X	heat exchanger
H_2O	water
ΔH	heat of fusion
J	joule
k	thermal conductivity
kg	kilogram
KHF_2	potassium bifluoride
l	liter
LCG	liquid cooling garment
LN_2	liquid nitrogen
m	meter
ml	milliliter
mm	millimeter
P	pressure
q	heat flow
t	thickness
T,t	temperature
Δt	temperature difference
UTRC	United Technologies Research Center
VAC	alternating current voltage
W	watt
x	cell thickness
Δ	difference, differential
ϵ	heat exchanger effectiveness
σ	standard deviation

PROGRAM PLAN

The effort covered by this program was intended to further develop and demonstrate the potassium bifluoride/water material as a viable thermal storage device. To this end, the program was divided into nine tasks to investigate various properties and characteristics of the potassium bifluoride/water material. These tasks are discussed in the following sections:

Materials Compatibility

Concentration Optimization

Effect of Wicking on Heat Absorption

Thermal Conductivity

Long Term Cycling

Volume Change with Temperature

Slurry Characteristics

Heat Sink Capacitance

Large Sample Testing

MATERIALS COMPATABILITY

The Materials Compatability task was undertaken to evaluate commonly utilized container materials to uncover a material or materials suitable for exposure to a highly saturated solution of potassium bifluoride (KHF_2) in water for use in heat absorbing system.

Initially, a literature and industry survey was conducted to screen for potential candidate materials. Actual industrial experience is quite limited. Two KHF_2 manufacturers, Harshaw Chemical Co. and American Hoechst Corp., could not recommend a metal with good resistance to KHF_2.

Five materials were selected for testing based on data available from various handbooks. Two sets of aluminum samples were prepared from AA 6061-T6. Both were chromic acid anodized per HS 334 Type I. One set was tested in the anodized condition and one was given two coats of Sherwin-Williams epoxy (H.S. 4675 Type I, V73VN31) per HS 3918. The three other candidate materials tested were Inconel 625, Hastelloy C and AISI 347.

Testing at room temperature was conducted over a five month period in which the samples were exposed to a solution of 30 g KHF_2/100 g distilled demineralized water. 1" x 3" test samples were made from sheet stock with a tungsten inert gas (TIG) weld centered longitudinally to simulate a welded assembly. The effect of mechanical stress on corrosion resistance, stress corrosion, was not included in the test program.

The KHF_2 solution, prepared in the ratio 30 g KHF_2 to 100 of water, was filtered prior to filling the plastic test containers. Each container held approximately 220 milliliters of solution. After filling the containers, the samples, one per container, were immersed and the tops affixed insuring an airtight seal.

All samples were visually inspected using an optical microscope at magnifications up to 40X. Table I summarizes the observations obtained after one, two, and five months of exposure. Weights were recorded before and after the exposure and the resulting changes are listed in Table II. Figures 1 through 5 show the effects on each of the samples of five months of exposure to KHF_2/H_2O solution.

The only significant corrosive attack noted occurred on the aluminum samples, coated and uncoated. The anodized coating provided only limited corrosion protection as evidence by areas of pitting (See Figure 1). The surface was a dull gray indicative of uniform attack, with some patches of white oxide. The

TABLE I

VISUAL OBSERVATIONS

Sample	KHF_2 Exposure		
	One Month	Two Months	Five Months
AA6061-T6 Anodized (t=.062")	Many white oxide patches with localized pitting	White oxide 10% surface; heavy pitting beneath	White oxide 5% surface; heavy pitting beneath
AA6061-T6 Anodized - Epoxy Ester (t=.062")	Coating blistered; heavy oxide; severe pitting	Coating blistered completely off 75% surface; heavy pitting	Coating no adhesion; heavy white, gray, reddish oxides
Inconel 625 (t=.062")	Dull gray surface oxide	Dull gray surface oxide	Dull gray surface oxide
Hastelloy C (t=.075"-.081")	Dull gray surface oxide	Dull gray surface oxide; some slight staining	Dull gray surface oxide
AISI 347 (t=.062")	Dull gray surface oxide	Dull gray surface oxide; some blackening on one side	Dull gray surface oxide; some staining on both sides

TABLE II

WEIGHT CHANGE AFTER FIVE MONTHS IN KHF_2

Sample	#	Exposure (months)	Initial Weight (grams)	Final Weight (grams)	% Weight \
Anodized Aluminum	1	1	14.930	14.931	0
	2	2	14.108	14.108	0
	3	5	14.166	14.168	0
Epoxy Ester Aluminum	7	1	14.734	15.245	3.5
	8	2	15.188	15.268	0.5
	9	5	13.027	13.212	1.4
Inconel	13	1	40.553	40.543	0
	14	2	39.044	39.045	0
	15	5	40.548	40.531	0
Hastelloy C	19	1	54.262	54.248	0
	20	2	53.081	53.075	0
	21	5	53.012	52.996	0
AISI 347	25	1	36.295	36.302	0
	26	2	37.093	37.098	0
	27	5	36.589	36.589	0

Figure 1 Anodized aluminum 1.6x

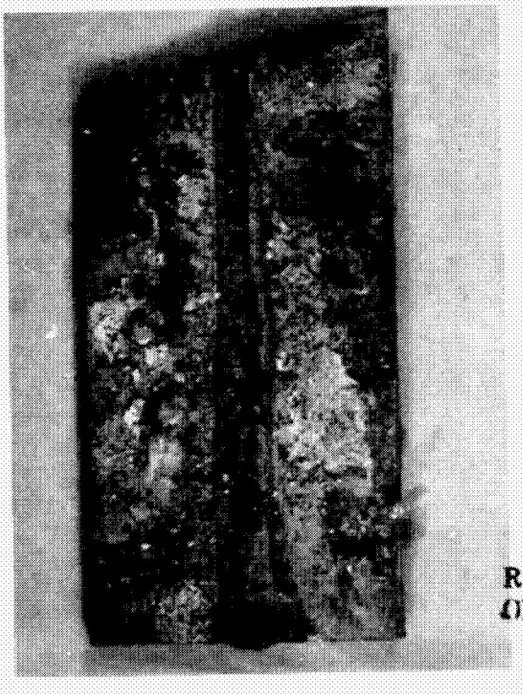

Figure 2 Epoxy ester coated anodized aluminum 1.6x

HAMILTON STANDARD Division of UNITED TECHNOLOGIES

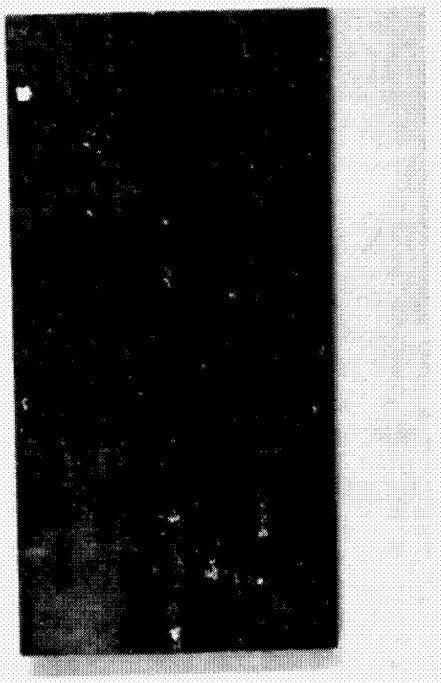

Figure 3 Inconel 625 1.6x

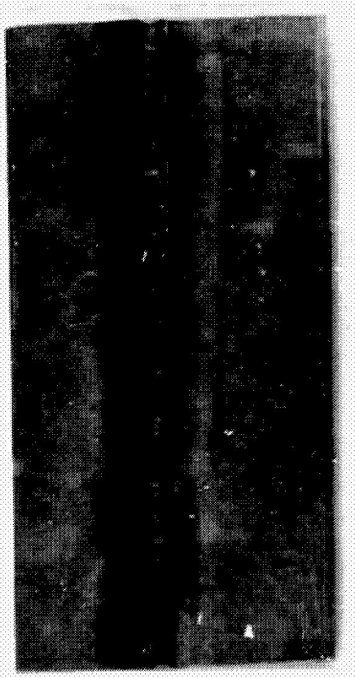

Figure 4 Hastelloy C-276 1.6x

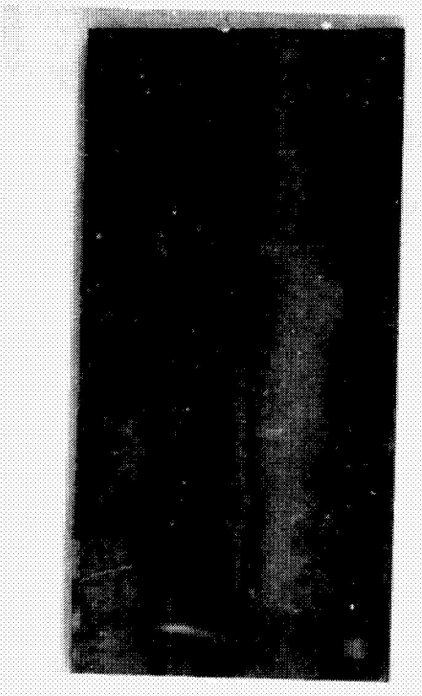

Figure 5 AISI 347 1.6x

epoxy ester coating did not retard the corrosion but actually accelerated the attack by creating a crevice cell effect. After five months, little coating was left on the sample. Severe pits with heavy oxide accumulations were observed after the first month. Figure 2 shows the surface condition after five months and Table II illustrates the weight increase due to oxide formation. Previous testing of uncoated unanodized AA 6061-T6 aluminum exposed to KHF_2 solution, performed during the Fusible Heat Sink for EVA Thermal Control Program, Contract No. NAS2-8912, produced a brightening or chemical polishing effect on the aluminum. Spectral analysis indicated a significant aluminum ion concentration in the remaining solution.

Hastelloy C, AISI 347, and Inconel 625 did not exhibit significant attack (See Figures 3, 4, and 5). Minor surface oxide was found on all three. Some slight differences are noted on Table I. However, each has exhibited excellent resistance to KHF_2/H_2O solution.

Based on the results of this material testing task, it has been concluded that the Hastelloy C, AISI 347, and Inconel 625 materials exhibit satisfactory resistance to KHF_2/H_2O solution corrosive attack at room temperature and below to justify their use in a heat absorbing system using KHF_2/H_2O solution.

Aluminum, either coated or uncoated, is considered unacceptable for exposure to KHF_2/H_2O solution due to the significant degradation observed.

CONCENTRATION OPTIMIZATION

The objective of the Concentration Optimization task was to measure the heat absorption of several concentrations of potassium bifluoride in water to determine the concentration that produces the maximum heat absorption per unit volume.

This task was conducted in two steps. First, the rotating bomb calorimeter used at United Technologies Research Center in previous studies of the heat sink capability of potassium bifluoride solutions was modified to increase the precision and reproducibility of the heat absorption measurements. Second, concentrations of 22, 25, 30, and 40 g KHF_2 per 100 g H_2O were measured in the rotating bomb to determine the concentration that yields the maximum heat storage.

ROTATING BOMB CALORIMETER MODIFICATION

The apparatus consists of a combustion bomb, calorimeter, thermometric system, power input measuring system, and liquid nitrogen cooling system. The calorimeter schematic is shown in Figure 6 and a photograph of the apparatus is shown in Figure 7. The bomb is capable of being rotated inside the calorimeter and thus is suited to measurements of heats of solution and mixing. The original stainless steel bomb has an internal volume of 331.8 ml (Paar Instrument Co. Catalogue No. 1004), teflon heat gasket and valve packing, and a Kel-F valve seat. All internal parts of the bomb are plated with 10 percent iridium-platinum. A platinum crucible containing the sample salt is mounted in an offset gimbal so that the bomb can be set at a 45° angle for filling. About 35 g of salt may be accommodated in the crucible. The calorimeter can surrounding the bomb contains about 2 liters of a 50-50 by volume methyl alcohol-water mixture that freezes at -100°C. During operation the bomb is completely immersed in this liquid which was kept at a known level for all runs by weighing the calorimeter can and contents before each run on a 5 kg capacity Seko 140 series balance. The calorimeter can also contains a stirrer, rotating mechanism, platinum resistance thermometer, and a 75 watt heater. The stirrer is operated at a constant 450 rpm using a belt drive from a synchronous motor. The rotation mechanism operates from a synchronous motor through a drive gear at a constant 10 rpm.

The thermometric system includes a platinum resistance thermometer of the flat calorimetric type (Leeds & Northrup type 8160B), a G-2 Mueller bridge (Leeds & Northrup type 8069B), and a high sensitivity galvonometer (Leeds & Northrup type HS2284d). The galvonometer is mounted on a Julius suspension and the light beam

FIGURE 6

SCHEMATIC OF ROTATING BOMB CALORIMETER

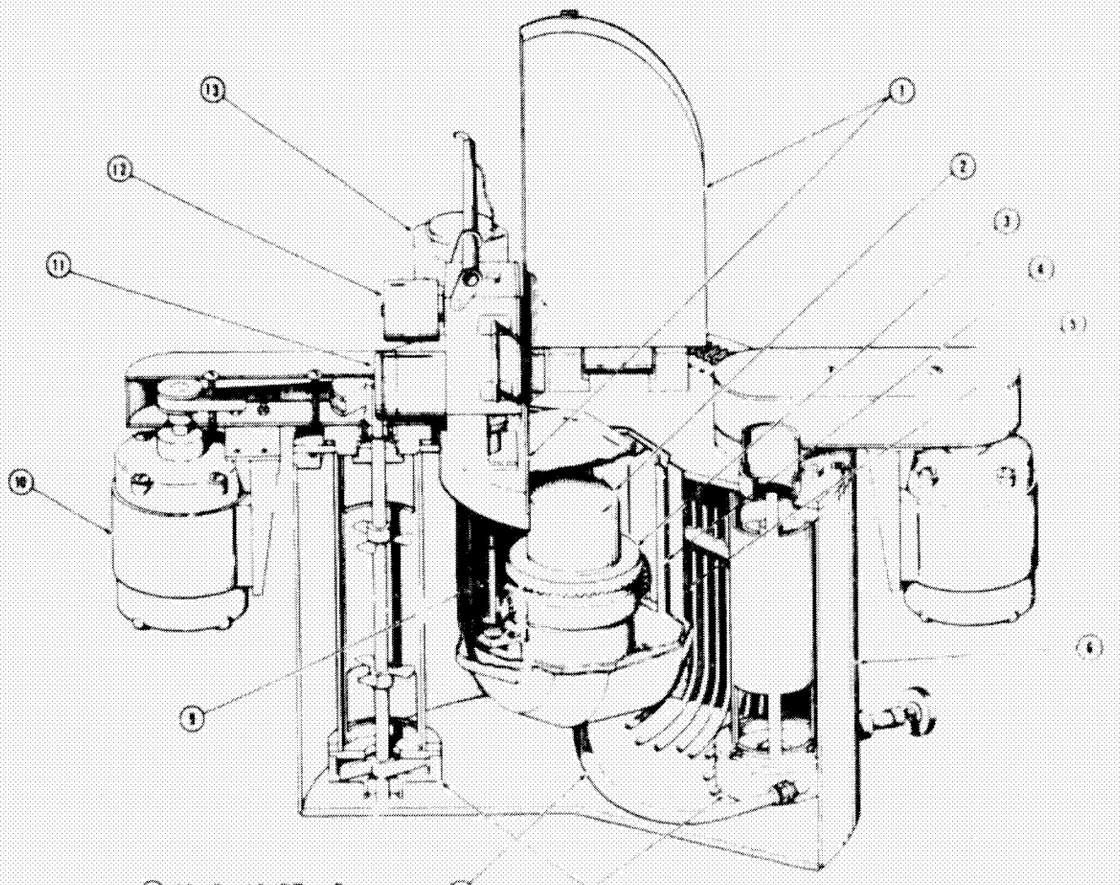

1. SPLIT JACKET LID
2. BOMB
3. ROTATING GEAR MECHANISM
4. CALORIMETER CAN
5. JACKET WELL
6. CALORIMETER JACKET
7. JACKET STIRRERS
8. LID WATER LINE
9. BOMB DRIVE SHAFT
10. JACKET STIRRER MOTOR
11. SYNCHRONOUS DRIVE MOTOR
12. POSITIONING SOLENOID
13. CALORIMETER CAN STIRRER MOTOR

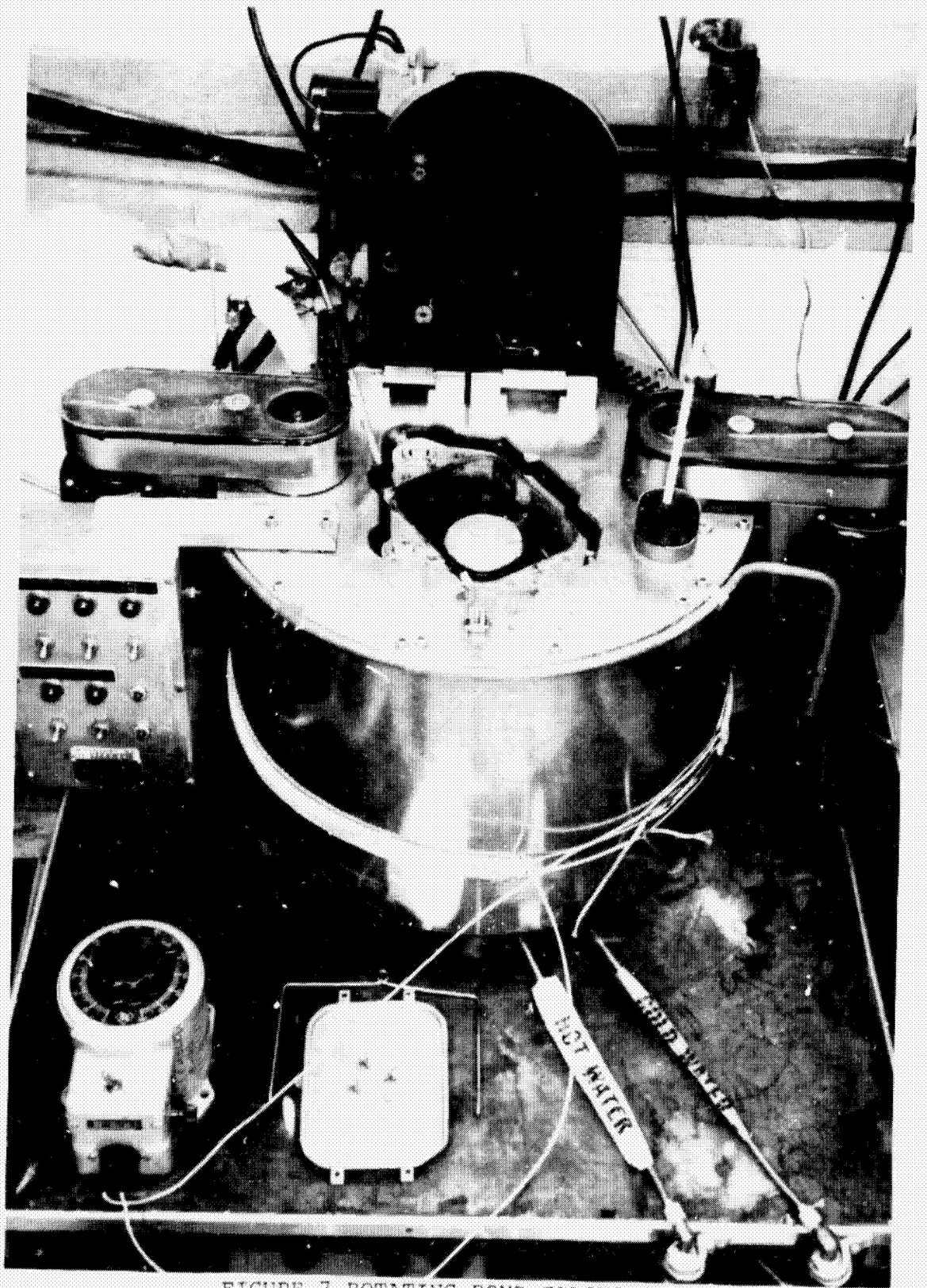

FIGURE 7 ROTATING BOMB CALORIMETER

is projected vertically over a path of two meters. Both the thermometer and bridge are periodically checked using a triple point cell and standard resistor. The sensitivity of this system is 0.001 °C/mm of galvonometer movement.

The calorimeter can is surrounded by a jacket containing 0.38 m^3 of fluid that completely enclosed it on all sides (see Figure 6). A 50 percent by volume methyl alcohol-water mixture is used in this jacket to minimize the heat flow to or from the calorimeter can; by adjusting the jacket fluid temperature to within 1°C of the calorimeter can temperature, the calorimeter is effectively under adiabatic conditions. A liquid nitrogen cooling system permits operation at jacket temperatures below 0°C. This system consists of a 50 liter dewar, a high pressure nitrogen bottle to pressurize the system, insulated polyflow tubing, and a copper tube suspended near the bottom of the jacket fluid. By forcing LN_2 through this system it is possible to reduce the jacket temperature from 20°C to -15°C in one hour. After the run has begun the jacket temperature is regulated manually by short bursts of LN_2 or by activation of heaters located within the jacket fluid.

The temperature of the calorimeter fluid in the can is lowered to the starting temperature for a run by the use of dry ice lumps, about 2.2 kg being sufficient to lower the temperature of the calorimeter fluid to -15°C. The temperature of the filled bomb is lowered by placing the bomb itself in a styrofoam chest surrounded by dry ice. The bomb is then placed in the calorimeter and allowed to come to temperature equilibrium with it. If this temperature is satisfactory for the run desired, then the jacket temperature is adjusted to within 1°C of the temperature of the calorimeter can whose value is monitored every two minutes as the run proceeds.

A cartridge heater immersed in the calorimeter fluid is used to raise the temperature of the bomb, its contents, and the calorimeter can and fluid to a temperature above that of the melting point of the water-ice or salt-ice mixture used in the bomb. The energy balance is:

$$\text{Electrical Energy in (J)} = \Delta T\,(C_{cal} + C_{bomb} + C_{fluid}) + \text{heat absorbed}$$

where C_{cal}, C_{bomb}, and C_{fluid} represents the heat capacity of the calorimeter can, the bomb and its contents, and the calorimeter fluid respectively, in J/°C, and ΔT is the temperature rise in °C, of the calorimeter. When the electrical energy applied to the calorimeter is not equal to the temperature rise term, then the difference represents a heat absorption process that is occurring in the bomb.

Several improvements in calorimeter operation and design have been incorporated into the present study, and these are described below. The schematic diagram in Figure 6 shows the bomb that was used in the previous study. This bomb was made of stainless steel and weighed 5.3 kg giving it a heat capacity of 2412 J/°C. One object of the present study was to reduce the heat capacity to the calorimeter fluid and the calorimeter bomb in order to decrease the calorimeter constant and increase the accuracy of the heat absorption measurements. The heat capacity of the calorimeter can has a value of 1.182 J/°C and is difficult to change. The calorimeter fluid is a mixture of methanol and water with a specific heat of 3.18 J/g°C. Enough of this fluid must be used to assure that heat is transferred from the electrical heater immersed in the fluid to the bomb. The amount of fluid that was found to be necessary to satisfy this condition was between 2,000 g and 2,300 g, giving the calorimeter fluid a heat capacity between 6,360 J/°C and 7,314 J/°C. The bomb used in the present study is made of brass, and weighs 1676 g. The heat capacity of this bomb is 637 J/°C, about one quarter the heat capacity of the original bomb previously used. The transfer of heat to the bomb contents is more rapid using a brass bomb rather than a stainless steel bomb because of the higher thermal conductivity of the brass. This tends to decrease the time required to melt the bomb contents and thus decreases the time dependent errors involved in the measurement. The calorimeter constant is the sum of the heat capacities of the calorimeter components and is generally between 8800 J/°C to 9800 J/°C, depending on the amount of calorimeter fluid present and the contents of the bomb. The specific heat of the contents of the bomb, about 100 g to 135 g of material, was assumed to be the same as the value for water, 4.18 J/g. Thus, the heat absorption measured for the contents of the bomb is the same as the specific heat of water. While this introduces a small error into the heat of fusion measurement of the salt-water mixture (an error which is not likely to exceed a few tenths of a joule per gram), it does not alter the comparison of the heat absorption of the salt-water system with that of water-ice.

A further improvement in the operation of the calorimeter was affected by the use of a watt-second meter that measures the electrical energy input to the calorimeter. This meter continuously integrates the power level with time and reads directly in joules, thus eliminating the error due to a fluctuating power level.

The operation of the calorimeter was checked by measuring the heat of fusion of water-ice. The results of these calibrating runs are shown in Table III. The calorimeter with the bomb

TABLE III

THE HEAT OF FUSION OF WATER-ICE

Run #	t_1 (°C)	t_2 (°C)	Δt (°C)	Bomb Contents (g)	ΔH (J/g)
1	-11.841	7.557	19.398	99.3	332
2	- 6.366	9.945	16.311	99.3	341
3	-11.376	8.970	20.346	99.4	350
4	-17.589	20.818	38.407	98.8	357
5	-16.717	22.438	39.155	98.8	323
6	-17.143	8.050	25.193	99.1	311
7	-16.599	8.425	25.024	99.1	335
8	-13.079	11.508	24.587	99.1	336
9	-13.524	11.242	24.766	99.1	354
10	-13.411	5.954	19.365	100.1	322
11	-11.646	8.969	20.615	100.1	340
12	-12.162	8.996	21.158	100.1	347

inside and the jacket surrounding the calorimeter (see Figure 6) were both brought down to the temperature t_1. The heater in the calorimeter was turned on at a level of 60 W when the temperatures in the calorimeter had stabilized for about 4 minutes. The temperature increase in the calorimeter was then followed closely with a platinum resistance thermometer and resistance bridge, while the jacket temperature was kept to within 1°C of the calorimeter can temperature to minimize heat leakage. At the final temperature, t_2, the heater had been turned off for several minutes and the temperature had again stabilized for 4 minutes. The amount of electrical energy introduced into the calorimeter was read on the watt-second meter, and the amount of energy it should have taken to raise the temperature of the calorimeter was calculated from the calorimeter constant and the known temperature increase. The difference between the expected energy required and the actual energy required is the heat absorbed by the phase change process occurring in the bomb. The last column in Table III lists the heat absorbed per gram for water-ice. These values give an average of 337 J/g, with a standard deviation, σ, of 14 J/g, which compares favorably to the accepted value of 333.5 J/g.

HEAT ABSORPTION MEASUREMENTS

The heat absorption of four different KHF_2 concentrations were measured in order to determine the concentration that exhibited the largest value of heat absorption. The results are shown in Table IV which also lists the starting and ending temperatures t_1 and t_2, the temperature difference Δt, and the weight of solution in the bomb. The average values for each concentration and the standard deviations for each concentration are listed in Table V. The largest value for the heat absorption was obtained for the concentration containing 25 g KHF_2 per 100 g of water, or a concentration of 20% by weight. These values are plotted against concentration in Figure 8. Included for comparison are the results for the 20 g KHF_2/100 g H_2O solution obtained in the previous study. The bars through these points represent the magnitude of the standard deviation.

It is evident from Figure 8 that the 20 percent by weight solution is very near the optimum and further refinement of this curve would not change the heat absorption by more than a few percent. The cooling effect of dissolving salt can be realized only up to the solubility limit of the KHF_2; it is not surprising that more concentrated solutions that do not fully redissolve at the final temperature fail to yield higher values for the heat absorption. However, if higher final temperatures were used in the calorimeter runs, the salt would make an additional contribution to the heat absorption at higher salt concentrations. In order to realistically assess the optimum concentration the final temperature was taken as about 10°C which would be the case in the actual use of a heat sink system for a personal cooling garment.

TABLE IV

HEAT ABSORPTION VERSUS KHF_2 CONCENTRATION IN WATER

Run #	Concentration (g/100 g H_2O)	Bomb Contents (g)	t_1 (°C)	t_2 (°C)	Δt (°C)	ΔH (J/g)
1	22	122.0	-17.146	11.112	28.258	477
2	22	122.0	-15.690	11.797	27.487	475
3	22	122.0	-16.662	11.587	28.249	492
4	22	122.0	-14.963	11.550	26.513	470
5	25	121.6	-17.868	9.589	27.457	520
6	25	121.6	-15.903	10.202	26.105	520
7	25	121.6	-14.547	9.997	24.544	510
8	25	121.6	-15.114	10.003	25.117	508
9	25	121.6	-16.657	10.313	26.970	545
10	25	121.6	-17.030	11.041	28.071	545
11	30	101.0	-14.041	11.878	25.919	505
12	30	101.0	-13.798	13.457	27.255	510
13	30	101.0	-13.622	14.091	27.713	516
14	30	101.0	-15.977	11.964	27.941	485
15	40	134.7	-16.380	10.759	27.139	464
16	40	134.7	-15.782	10.769	26.551	482
17	40	134.7	-15.406	9.958	25.364	436
18	40	134.7	-15.792	10.541	26.333	481
19	40	134.7	-19.305	10.898	30.203	450
20	40	134.7	-16.388	9.747	26.135	481

TABLE V

AVERAGE HEAT ABSORPTION AND STANDARD DEVIATION

Concentration (g KHF /100g H_2O)	Average Heat Absorption (J/g)	(J/cm^3)	Standard Deviation (J/g)	(J/cm^3)
0 (Pure Water)	333.5	333.5	-	-
22	479	541	9	10
25	525	604	17	20
30	504	595	13	15
40	466	578	19	24

FIGURE 8

HEAT ABSORPTION OF KHF_2/WATER SOLUTIONS

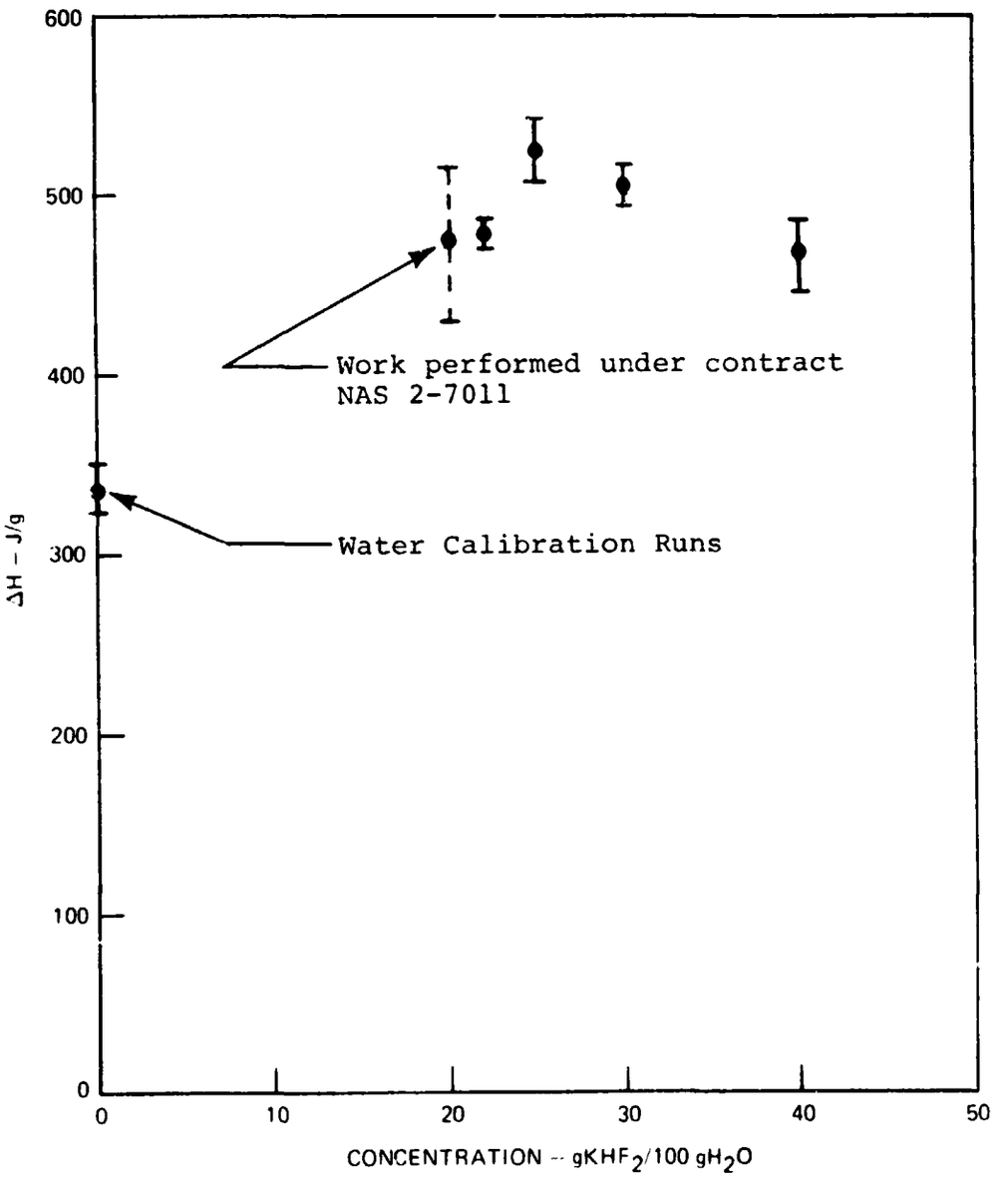

EFFECT OF WICKING ON HEAT ABSORPTION

The wicking effect task was performed to evaluate any anomalies that might occur in heat absorption capacity of the potassium bifluoride in water due to containment of the solution in a wick media.

Calorimeter measurements were made using pure water completely absorbed in wicking material. The wicking material used during this task is the #67 dacron felt wick material used to contain water in the ice pack hardware manufactured and tested under NASA Ames Research Center contract NAS 2-7011. These runs, listed in Table VI, averaged 333 $\pm$ 9 J/g, very close to the accepted literature value of 333.5 J/g, and compare closely to the 337 $\pm$ 14 J/g reported in Table III for water-ice in the absence of wicking material. These results indicate there is nothing inherent in the wick material that would change the results of the calorimeter runs for KHF_2 solutions.

The heat absorbed by a solution of 25 g KHF_2 per 100 g H_2O completely contained in the felt wicking material is shown in Table VII. These runs averaged 360 J/g with a standard deviation of 27 J/g, compared to 525 $\pm$ 17 J/g reported in Table V for this concentration without the use of felt wick. An examination of the wick after these calorimeter runs revealed undissolved salt crystals on the surface of the wick material. The calorimeter runs without wicking did not exhibit undissolved salt at the final temperature at this KHF_2 concentration; therefore, it was concluded that the wicking material inhibits the redissolution of the salt during thawing. It is possible that a certain amount of bulk liquid motion must be allowed in order for the salt to dissolve in a reasonable time. The small amount of liquid motion caused by convection currents from temperature and concentration gradients contributes to the redissolution process without wicking. Also, liquid movement in the unwicked solution that is caused by ambient vibration from the stirring motors is inhibited by the felt wick.

A second contributing factor affecting the wicked heat absorption is associated with the freeze rate of the KHF_2/H_2O solution, as described in the Large Sample Testing section. It is possible that an additional effect on heat absorption occurs as a result of the decreased heat transfer caused by the wick material.

Based on the results of this testing it must be concluded that the heat absorption capacity of potassium bifluoride in water is severely decreased when contained in a dacron felt wick media.

TABLE VI

EFFECT OF WICKING MATERIAL ON HEAT ABSORPTION OF WATER-ICE

Run #	t_1 (°C)	t_2 (°C)	Δt (°C)	Bomb Contents (g)	ΔH (J/g)
1	-9.486	10.044	19.530	100	322
2	-8.846	9.638	18.484	100	336
3	-10.773	9.773	20.546	100	340

TABLE VII

EFFECT OF WICKING MATERIAL ON HEAT ABSORPTION OF KHF_2 SOLUTIONS

Run #	t_1 (°C)	t_2 (°C)	Δt (°C)	Bomb Contents (g)	ΔH (J/g)
1	-15.071	8.623	23.694	120	379
2	-15.368	10.069	25.437	120	322
3	-14.262	10.436	24.698	120	384
4	-14.606	9.982	24.588	120	374
5	-17.181	10.091	27.272	120	341

THERMAL CONDUCTIVITY

The thermal conductivity task was undertaken to measure thermal conductivity of the 20 percent KHF_2/H_2O solution (25 g KHF_2 per 100 g H_2O) in the liquid and the solid phase, and in the unwicked and the wick contained states.

Thermal conductivity measurements were accomplished using the "heat flow meter" method, the apparatus for which is shown schematically in Figure 9. In this technique, the heat flow across the sample is measured by a thin sensor consisting of a multi-junction thermocouple for which the voltage output is proportional to the heat flow through it. A Kiethley Model 860 Heat sensor is placed on one side of the cell and held in place by an extremely thin double sided adhesive tape. The same energy must pass through the sensor as through the surface of the cell and, thus, the heat flow is measured directly. The thermal conductivity k, temperature difference Δt, cell thickness x and heat flow q are related according to

$$k = \frac{xq}{\Delta t}$$

where the units for k are in W/m^oC, q is in W/m^2. x is in m, and Δt is in ^oC. In order to avoid the introduction of an error due to convective heat transfer, the cell is 5mm in thickness. This thickness and the fact that the top of the cell was always kept at a higher temperature, assuring the highest density liquid was on the bottom, is enough to prevent significant convection from occurring. (Ref.: "Diffusion and Heat Flow in Liquids," H. J. V. Tyrrell Buttersworths, London (1961), p. 294).

Tables VIII, IX, and X contain the calibration results for water, ice, and quartz, respectively. The average of these results and the standard deviations are given in the summary Table XVII. The results for these three calibrating substances show reasonable agreement with values published in the literature. For water the published value is 0.615 W/m^oC, for ice the published value is 2.38 W/m^oC, and for quartz the published value is 1.56 W/m^oC. Tables XI and XII show the data for the optimum solution; the mean values and standard deviations are shown in Table XVII. The next two tables, XVIII and XIX, show results of calibration runs using water and ice for the optimum KHF_2 solution in wicking material. The mean values and standard deviations for these tests are presented in Table XVII.

The optimum KHF_2 solution, with 25 g of salt dissolved in 100 g of water, exhibited a thermal conductivity of 0.535 W/m^oC. This conductivity is about 86 percent of the value obtained for water,

FIGURE 9

THERMAL CONDUCTIVITY APPARATUS

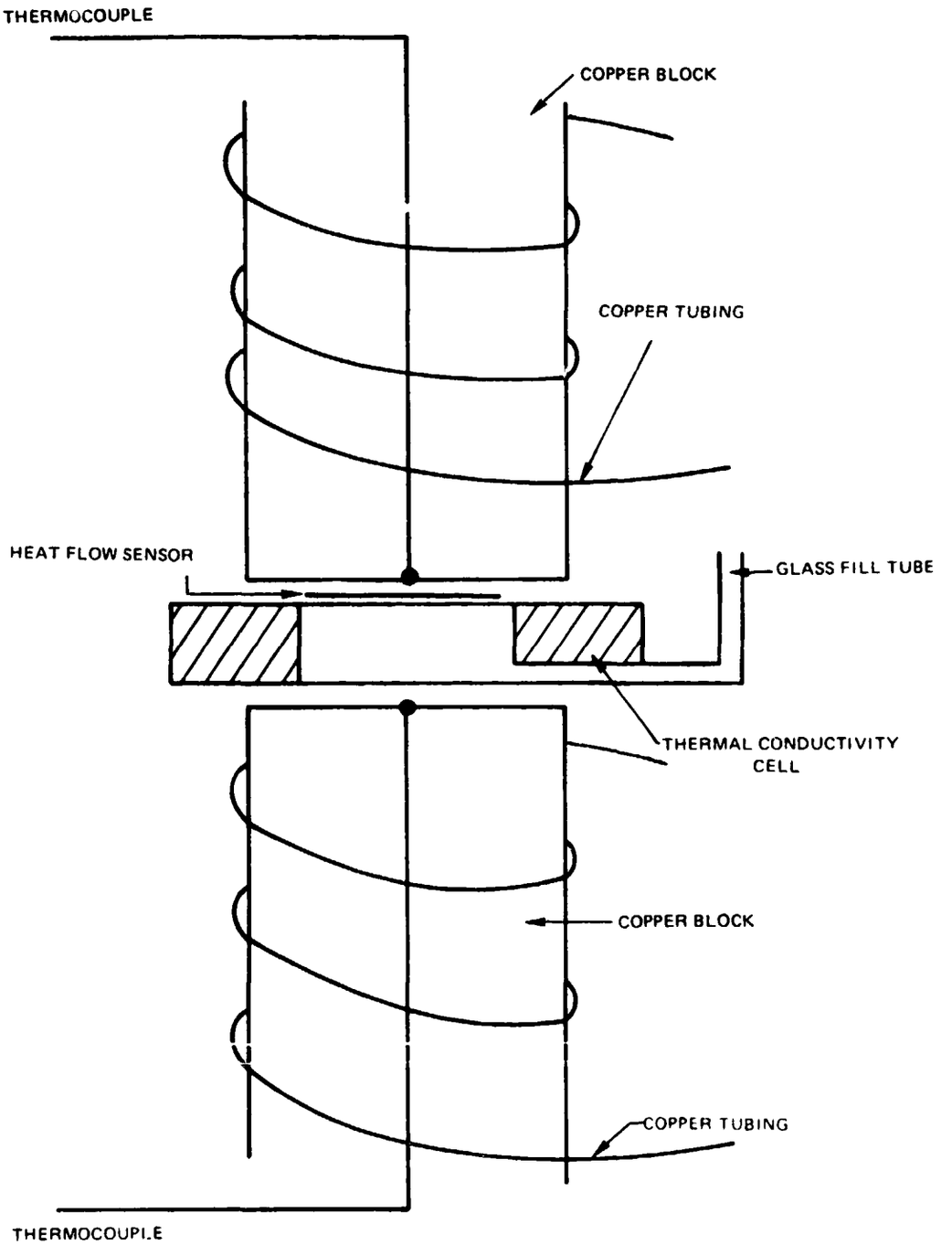

while the frozen solution at 2.31 W/m^{o}C is 98 percent of the value obtained for ice.

The measurements on these solutions when absorbed in wicking material were somewhat ambiguous, since the value for ice with wicking was much lower than that for ice without wicking, while the value for water with wicking was higher than for water without wicking. For the salt absorbed in wicking the values for both liquid and frozen forms were lower than for without wicking as would be expected if the wick material retards the transfer of heat through the thermal conductivity cell.

TABLE VIII

THERMAL CONDUCTIVITY OF WATER

t_1 °C	t_2 °C	Δt °C	q W/m²	k W/m°C
30.0	42	12	1463	0.609
29.9	41.4	11.5	1423	0.619
30.1	41.4	11.3	1392	0.616
30.5	41.5	11.0	1353	0.615
30.7	39.9	9.25	1126	0.608
30.8	39.5	8.75	1087	0.621
30.8	39.3	8.50	1048	0.617
30.9	35.6	4.75	602	0.634
30.5	35.0	4.50	594	0.662
30.7	34.9	4.25	532	0.627
31.2	34.9	3.75	469	0.626

TABLE IX

THERMAL CONDUCTIVITY OF ICE

t_1 °C	t_2 °C	Δt °C	q W/m²	k W/m°C
-49.4	-1.9	47.5	21743	2.29
-37.7	-1.4	36.3	17285	2.38
-32.0	-0.7	31.3	14782	2.36
-27.5	0	27.5	13140	2.39
- 5.6	-1.7	3.88	1768	2.28
- 4.7	-0.7	4.00	1846	2.31
- 4.3	-0.3	4.00	1932	2.42

TABLE X

THERMAL CONDUCTIVITY OF QUARTZ

t_1 °C	t_2 °C	Δt °C	q W/m²	k W/m°C
26.9	30.0	3.13	1072	1.71
28.3	40.0	11.8	3845	1.63
26.0	39.0	13.0	4287	1.65
26.3	38.8	12.5	4129	1.65

TABLE XI

THERMAL CONDUCTIVITY OF 25 g KHF_2/100 g H_2O SOLUTION

t_1 °C	t_2 °C	Δt °C	q W/m²	k W/m°C
29.0	42.7	13.75	1502	0.546
29.0	43.0	14.0	1541	0.550
28.6	43.1	14.5	1580	0.545
28.9	36.4	7.5	751	0.500

TABLE XII

THERMAL CONDUCTIVITY OF 25 g KHF_2/100 g H_2O SOLUTION - FROZEN

t_1 °C	t_2 °C	Δt °C	q W/m²	k W/m°C
-73	-15.5	57.5	26428	2.30
-66.5	-14.0	52.5	24723	2.35
-55.0	-25.0	30.0	13640	2.27
-44.1	-16.6	27.5	12788	2.33
-37.8	-13.8	24.0	11083	2.31
-26.5	-12.0	14.5	6734	2.32

TABLE XIII

THERMAL CONDUCTIVITY OF WATER IN WICK

t_1 °C	t_2 °C	Δt °C	q W/m²	k W/m°C
25.3	37.0	11.8	1879	0.796
25.5	37.0	11.5	1879	0.817
25.9	36.9	11.1	1838	0.828
26.5	34.4	7.88	1330	0.844
26.1	33.[illegible]	7.50	1214	0.809
25.8	32.0	6.20	1024	0.826
26.2	31.7	5.5	883	0.802
26.4	31.1	4.68	750	0.801
26.4	30.6	4.25	671	0.790

TABLE XIV

THERMAL CONDUCTIVITY OF ICE IN WICK

t_1 °C	t_2 °C	Δt °C	q W/m²	k W/m°C
-56.5	-6.5	50.0	6808	0.608
-47.8	-4.0	43.8	6209	0.710
-42.5	-1.2	41.3	5831	0.706
-30.0	0	30.0	4098	0.684
-14.9	-0.6	14.3	1891	0.661
-11.5	-1.7	9.75	1440	0.738
- 6.8	-4.8	2.0	274	0.684
- 5.8	-3.5	2.25	328	0.730
- 5.3	-2.8	2.50	416	0.829
-17.5	-2.0	15.5	2301	0.742
-13.6	-4.6	9.0	1368	0.760

TABLE XV

THERMAL CONDUCTIVITY OF 25 g KHF_2/100 g H_2O SOLUTION IN WICK

t_1 °C	t_2 °C	Δt °C	q W/m²	k W/m°C
26.9	29.7	12.8	1125	0.440
26.8	39.4	12.6	1087	0.431
27.2	37.5	10.3	898	0.437
27.1	36.2	9.13	791	0.433
26.8	35.5	8.5	760	0.446
26.9	34.4	7.55	681	0.451
26.9	33.4	6.5	611	0.469
26.9	32.4	5.50	533	0.484
26.6	30.8	4.25	422	0.497

TABLE XVI

THERMAL CONDUCTIVITY OF 25 g KHF_2/100 g H_2O SOLUTION IN WICK - FROZEN

t_1 °C	t_2 °C	Δt °C	q W/m²	k W/m°C
-37.8	-7.8	30.0	6115	1.02
-31.3	-5.0	26.3	5295	1.01
-20.1	-13.8	6.3	1182	0.937

HAMILTON STANDARD Division of United Technologies

TABLE XVII

SUMMARY OF THERMAL CONDUCTIVITY DATA

Solution	k (W/m°C)
Water (Published)	0.615
Water (Experimental)	0.623 ± 0.015
Ice (Published)	2.38
Ice (Experimental)	2.35 ± 0.05
Quartz (Published)	1.56
Quartz (Experimental)	1.66 ± 0.03
25 g KHF_2/100 g H_2O	0.535 ± 0.024
25 g KHF_2/100 g H_2O - Frozen	2.31 ± 0.03
Water in wick	0.813 ± 0.018
Ice in wick	0.720 ± 0.047
25 g KHF_2/100 g H_2O in wick	0.454 ± 0.024
25 g KHF_2/100 g H_2O in wick - frozen	0.989 ± 0.045

LONG TERM CYCLING

The purpose for conducting the long term cycling task was to uncover any anomalies that might have occurred as a result of long term freeze/thaw cycling of the KHF_2/H_2O solution.

In the work covered under Contract NAS 2-7011. the maximum number of freeze-thaw cylces undergone by a single solution was four. There was no apparent change in thermal absorption properties noted.

The heat absorbed by the 20 g KHF_2 per 100 g H_2O solution was measured as a function of the number of freeze/thaw cycles with measurements taken after 1, 10, 20, 40, and 50 cycles. The number of cycles reported do not include those that were used for the heat absorption measurements and, therefore, the actual number of cycles are somewhat greater than the nominal values in Table XVIII.

The heat absorption measurements shown in Table XVIII for the single cycle case were taken on a fresh solution of 25 g KHF in 100 g of water. The second series of heat absorption measurements were taken after the bomb had been frozen and thawed ten more times. The third series of measurements were taken after a total of twenty freeze-thaw cycles not including those cycles needed for the heat absorption measurements. A single heat absorption measurement was made after completion of the fourth set of freeze-thaw cycles. This fourth series of planned runs was abbreviated to only one valid measurement due to equipment failure. The heater surrounding the jacket failed to keep the jacket and calorimeter at the same temperature, and, therefore, the initial results were suspect and were not tabulated. Only one determination, made after the heater was replaced, is reported in Table XVIII. The fifth series of runs were taken after ten more freeze-thaw cycles bringing the actual total of cycles to seventy including those used for the heat absorption measurements.

As Table XVIII indicates, there was no statistically significant change in the heat absorption over the entire course of the measurements. The total number of measurements, fourteen, can be combined to give a grand mean value of 533 J/g with a standard deviation of 17 J/g.

TABLE XVIII

LONG TERM CYCLING HEAT ABSORPTION

# of Cycles	Determination of ΔH (Joules/g)	Average ΔH (J/g)	Standard Deviation (J/g)
1	523, 560	542	26
10	549, 529, 515	531	17
20	533, 525, 538, 520	529	8
40	545	545	-
50	497, 530, 560, 543	533	27

VOLUME CHANGE WITH TEMPERATURE

The volume change task was performed to determine the freeze/thaw volume change, the liquid thermal expansion characteristics, and the solid thermal expansion characteristics of the 25 g KHF_2 per 100 g H_2O solution.

FREEZE/THAW VOLUME CHANGE

The freeze/thaw apparatus was constructed by modifying the thermal conductivity cell shown in Figure 9. The inside diameter of the glass tube standpipe was measured so that its volume per unit length is known. The copper blocks established the required freezing temperature by circulation of liquid nitrogen through the copper tubing.

The cell was filled, first with H_2O and then with a solution of 25 g KHF_2 per 100 g H_2O, carefully avoiding the presence of air bubbles and leaving liquid visible in the glass tube. The solution freezing in the cell forced liquid up the tube, the volume increase being proportional to this distance. The amount of liquid in the cell was determined by weighing the cell before and after the filling.

The volume change on melting for the water measurements averaged 0.089 $cm^3/g \pm 0.008$ cm^3/g. This compares well to the literature value (International Critical Tables) of 0.090 cm^3/g. The volume change on melting for the KHF_2/H_2O solution averaged 0.083 $cm^3/g + 0.004$ cm^3/g which translates to 0.095 $cm^3/cm^3 \pm$ 0.005 cm^3/cm^3. The value on a volume basis is slightly larger than water, the value on a weight basis is about the same as that for water.

LIQUID THERMAL EXPANSION

Thermal expansion testing was accomplished using the thermal conductivity cell from the freeze/thaw apparatus. The cell was filled as before with the appropriate solution and placed in a constant temperature bath. The bath temperature was varied from 22°C to -20°C by bubbling liquid nitrogen into the bath. The specific volume of water was measured first to check the technique, and the results are shown in Figure 10. The specific volume for water is plotted vs. temperature for temperatures ranging from 0°C to 30°C with the symbol X used for the values from Lange's Handbook of Chemistry, and the symbol 0 used for the measured values. Both sets of points lie on the same curve and show the characteristic minimum specific volume at about 4°C. The change in specific volume with temperature for water

FIGURE 10

SPECIFIC VOLUME VS TEMPERATURE FOR WATER

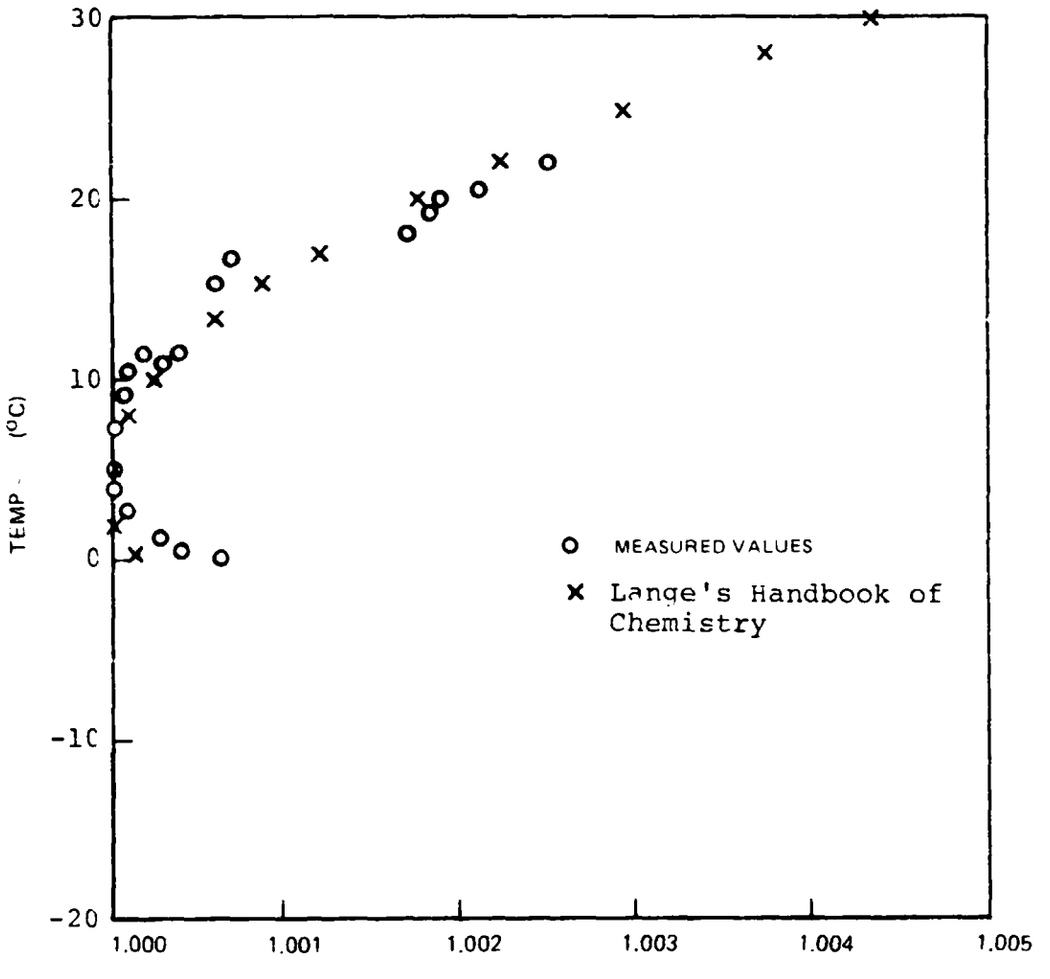

is quite dependent on temperature, especially in the temperature range between 0°C and 10°C. Figure 11 shows the data obtained for the KHF_2 solution. This curve shows a minimum in the specific volume at about 1°C - 2°C with a fairly constant slope between 25°C and 3°C of 1.74×10^{-4} $cm^3/cm^3°C$. This compares to approximately 2.55×10^{-4} $cm^3/cm^3°C$ for water between 20°C and 30°C, and approximately 1.60×10^{-4} $cm^3/cm^3°C$ for water between 10°C and 20°C. The interpretation of the measurement for the KHF_2 solution is complicated by the fact that the solubility decreases drastically with temperature, so that some salt or salt hydrate is coming out of solution at low temperatures. It would appear, the salting out effect notwithstanding, that the change in density with temperature for the KHF_2 solution is not much different from that for water.

SOLID THERMAL EXPANSION

In this determination, the cell was first half filled with the solution, which was then frozen to anchor the liquid to the bottom of the cell. The remaining volume of the cell was taken up by mercury which also was present in the fill tube. As the temperature of the copper blocks is changed the extent of expansion of the frozen KHF_2 solution and the mercury is reflected in the level of mercury in the fill tube. The apparatus was calibrated with ice between the temperatures of -32.2°C and -10.7°C. The known weight of ice and of mercury, and the volume coefficient of thermal expansion for mercury were used to calculate a coefficient of thermal expansion for ice of 0.000131 $cm^3/cm^3°C$. This value compares closely to the published value from the International Critical Tables of 0.000159 $cm^3/cm^3°C$ at -10.0°C and 0.000102 $cm^3/cm^3°C$ at - 25.0°C.

The volume coefficient of expansion for the frozen KHF_2 solution between the temperatures of -14.8°C and -31.5°C was determined to be 0.000102 $cm^3/cm^3°C$. This value is very similar to that for ice. The density of the frozen KHF_2 solution was measured as 1.03 g/cm^3 at -15.0°C compared to 0.917 g/cm^3 for ice at 0°C.

FIGURE 11

SPECIFIC VOLUME VS TEMPERATURE FOR THE OPTIMUM SOLUTION (20% KHF_2 IN WATER)

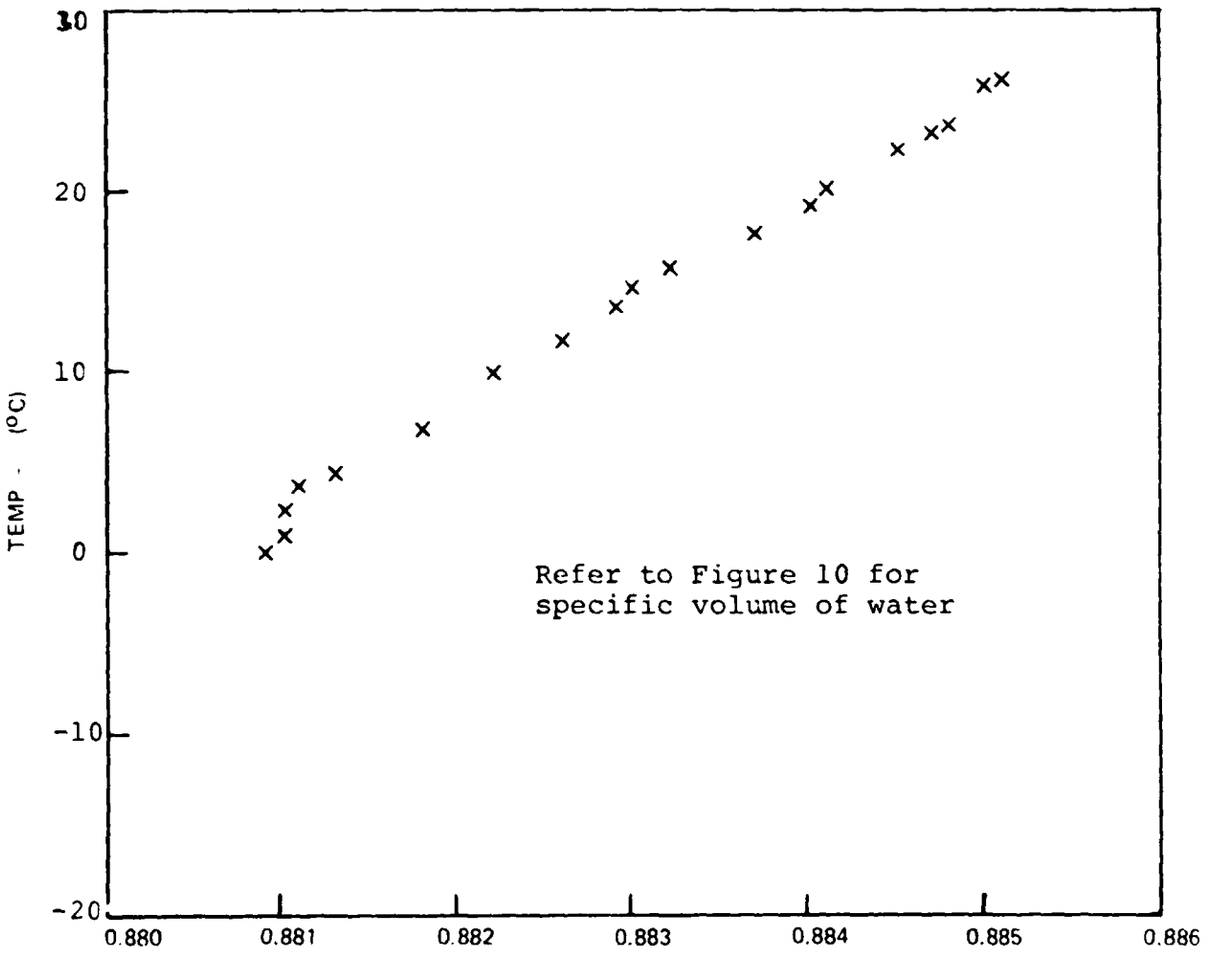

SLURRY CHARACTERISTICS

The objective of this task is to determine the heat absorption, thermal conductivity, and thermal expansion properties of a slurry formed by mixing 10 percent by volume of ethanol with 90 percent by volume of the 25 g KHF_2 per 100 g H_2O bifluoride solution. The significance of this mixture is its composition in the -17.8°C range. When the freezing point of the slurry is reached, approximately -9°C, the slurry starts to freeze and the ethanol separates from the frozen portion, thereby increasing the ethanol concentration in the unfrozen mixture to a point where it will not freeze. As the temperature continues to lower, additional slurry freezes, the ethanol concentration in the unfrozen slurry increases, and the volume of the unfrozen slurry decreases. When the terminal temperature of -17.8°C is reached the unfrozen portion is relatively highly concentrated ethanol located in a central region furthest away from the cooling heat sink. By locating a circulating source in the unfrozen area the slurry can be circulated to a heat exchanger. This configuration produces a heat sink system with a significant reduction in volume when compared to a conventional regenerable metal to metal contact type.

HEAT ABSORPTION

The heat absorption per gram of the slurry was expected to be about 7 percent lower than that of the KHF_2/H_2O solution, since the dilution with ethanol of 10 percent by volume results in a 7 percent increase in weight for, presumably, the same heat absorption. The heat absorption average for the four runs in Table XIX was 467 $\pm$ 13 J/g, 12 percent lower than the heat absorption for the optimum solution. The slightly lower than expected heat absorption value most likely can be attributed to the fact that a portion of the KHF_2 remained dissolved in the unfrozen portion of the fully chilled slurry.

THERMAL CONDUCTIVITY

The thermal conductivity data for the slurry are listed in Tables XX and XXI. Adding the ethanol to form a 10 percent by volume slurry did not significantly change the liquid thermal conductivity from that for the pure solution, 0.548 W/m°C compared to 0.535 W/m°C.

In measuring the thermal conductivity of the frozen slurry, it must be recognized that the slurry was not completely frozen at the temperatures of measurement and liquid was present across the temperature gradient of the cell, causing the thermal conductivity of the slurry at low temperatures to be only 0.841 W/m°C, 157 percent of the unfrozen slurry value, and 36 percent of the frozen KHF_2/H_2O solution. The thermal conductivity of the frozen slurry is highly dependent upon the location of

TABLE XIX

HEAT ABSORPTION OF SLURRY

Run #	t_1 (°C)	t_2 (°C)	Δt (°C)	Bomb Contents (g)	ΔH (J/g)
1	-21.114	10.301	31.415	133.5	454
2	-13.202	10.301	23.503	133.5	458
3	-18.984	9.558	28.542	133.5	476
4	-19.078	10.281	29.359	133.5	481

TABLE XX

THERMAL CONDUCTIVITY OF SLURRY

t_1 (°C)	t_2 (°C)	Δt (°C)	q (W/m^2)	k ($W/m°C$)
25.9	31.2	5.3	596	0.561
25.7	39.4	13.8	1541	0.558
25.7	39.2	13.5	1463	0.542
26.1	38.6	12.5	1352	0.541
26.2	28.2	12.0	1289	0.538
26.6	37.8	11.8	1236	0.547
26.7	37.4	10.8	1166	0.540
26.6	37.1	10.5	1166	0.555
			Average	0.548

TABLE XXI

THERMAL CONDUCTIVITY OF COLD SLURRY

t_1 (°C)	t_2 (°C)	Δt (°C)	q (W/m^2)	k ($W/m°C$)
-78.9	- 3.9	75.0	14562	0.970
-74.1	- 5.3	68.8	12450	0.904
-59.1	- 7.0	52.5	8290	0.790
-59.1	-22.4	23.8	3972	0.831
-39.5	-19.7	19.8	3278	0.826
-32.0	-17.0	15.0	2408	0.803
-26.1	-13.8	12.3	2002	0.814
-19.1	- 9.8	9.25	1510	0.816
-14.8	- 7.0	7.75	1463	0.944
-59.6	-10.8	48.8	7533	0.772
-68.1	-23.1	45.0	7218	0.803
-61.5	-24.2	36.3	6115	0.844
-57.6	-23.0	28.8	4823	0.836
-41.8	-19.3	22.5	3688	0.822
			Average	0.841

the liquid portion; the thermal conductivity of the fully frozen portion of the slurry most likely approaches that of the frozen KHF_2/H_2O solution.

THERMAL EXPANSION PROPERTIES

Specific volume, the reciprocal of density, of the slurry is plotted against temperature in Figure 12. The maximum density is reached at 0°C and the onset of freezing occurs at -9°C. The solution continues to expand rapidly until a temperature of about -19°C, where the expansion rate levels off.

FIGURE 12

SPECIFIC VOLUME VS TEMPERATURE FOR THE SLURRY
(20% KHF_2 IN WATER + 10% BY VOLUME ETHANOL)

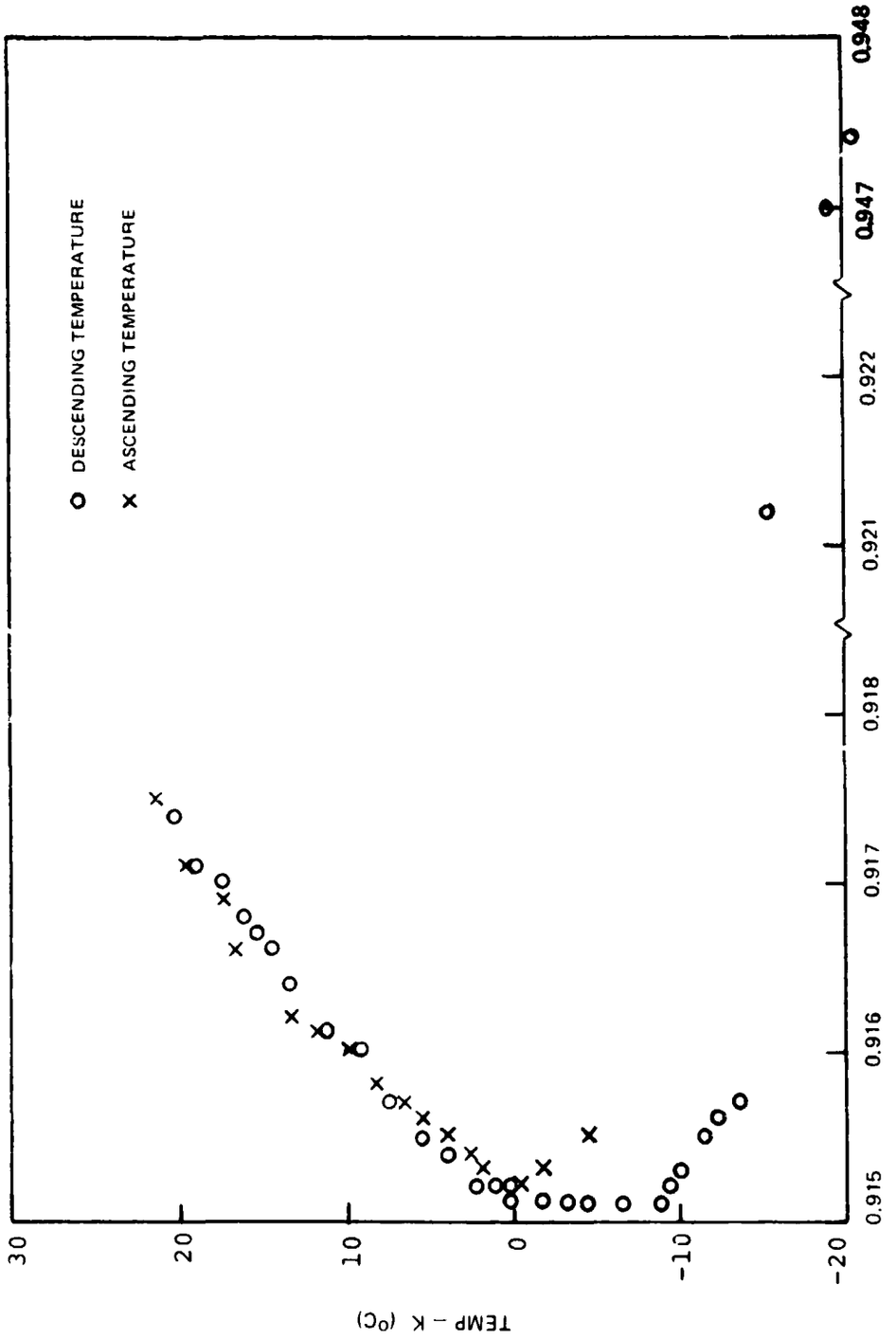

HEAT SINK CAPACITANCE

Full scale performance tests were conducted to evaluate the heat sink capacitance of a frozen mixture of potassium bifluoride (KHF_2) and water. As a test bed, the prototype ice pack heat sink subsystem was employed to provide a convenient means of data acquisition.

When KHF_2 is added to water, an initial exothermic hydration occurs followed by bn endothermic dissolution of the hydrated salt. Literature values for the heat of solution report the net energy absorbed by the dissolving system, and do not separate the hydration and solution effects. Regeneration is accomplished by a simple cooling and freezing of the system since the salt precipitates (as hydrate) as the water freezes. Testing was required to determine the available heat sink capacitance when starting with the hydrated salt and ice. United Technologies Research Center calorimeter results have indicated a 50 percent by weight improvement over a pure water system.

The test program performed under this task compared the heat absorption capability of an ice chest (freeze/thaw mode) containing distilled water with the heat absorption capability of the same ice chest (freeze/thaw mode) containing a mixture with a concentration of 25 g KHF2 per 100 g H_2O.

In the test set-up, illustrated in Figure 13, water, representing the liquid cooling garment (LCG) transport loop, passes through the ice chest heat exchanger; is cooled by the melt process; returns to the LCG simulator (a heater in the test system) where is picks up the metabolic energy; and returns to the heat exchanger. A transport loop bypass around the ice chest permits temperature control of the LCG (heater) inlet. The test plan is included in Appendix A. Test evaluation is most convenient at a metabolic load of 439 watts (1500 Btu/hr) with the transport loop inlet to the LCG (test heater) controlled to 21°C (70°F). Water flow through the ice chest H/X starts low and slowly increases as the ice melts and the thermal resistance between the H/X and ice/liquid interface grows. When all the ice is melted or when the thermal resistance grows so large that the transport loop cannot be controlled to 21°C (70°F), the test is terminated - usually 60 to 90 minutes of run time.

As the flow through the H/X increases, the heat exchanger effectiveness, ϵ, decreases in accordance with the following equation:

$$\epsilon = \frac{\text{LCG water inlet temperature - LCG water outlet temperature}}{\text{LCG water inlet temperature - melting point temperature of sink material}}$$

Plots of effectiveness versus cumulative heat transfer (or cumulative heat transfer divided by 439 watts (1500 Btu/hr) the original specification energy storage requirement) can be used to graphically portray heat sink exhaustion. Beyond an effectiveness of 0.4 to 0.5, little additional energy is

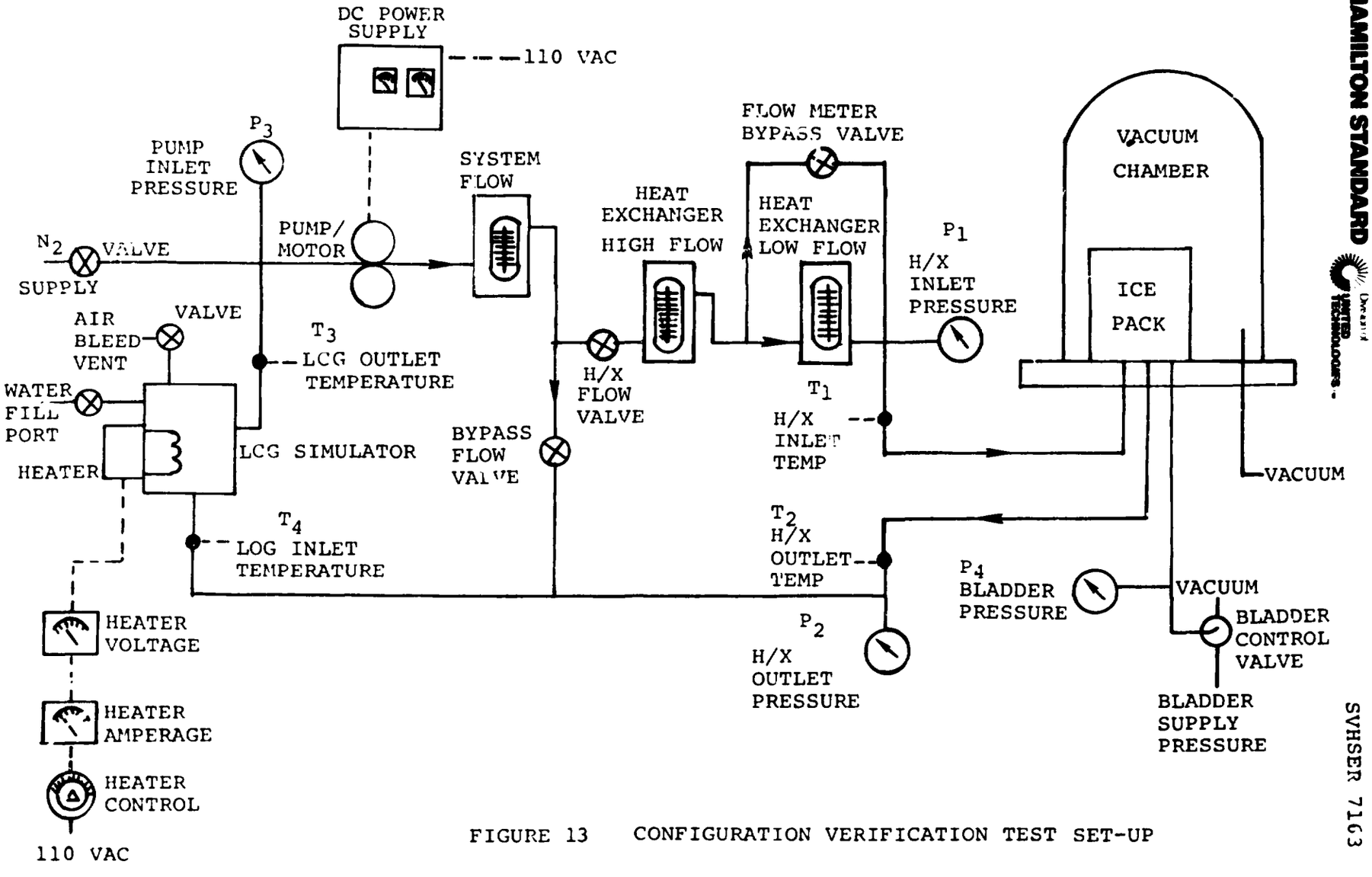

FIGURE 13 CONFIGURATION VERIFICATION TEST SET-UP

removed from the ice chest and ϵ rapidly drops to zero. Relative comparisons at $\epsilon = 0.5$ provide a measure of the total heat sink capacity of one run versus another.

Representative data from this test series are shown in Figures 14 and 15, and are compared to the original water data obtained October 3, 1974, Curve I. Curve II also used distilled water (April 28, 1976) but exhibited an approximate 14 percent increase in heat capacity. This variation is within the range anticipated and Curve II was used as the baseline. Four runs using the KHF_2/H_2O solution are discussed in the following paragraphs. Test log sheets are included in Appendix B.

WICKED KHF_2/H_2O SOLUTION

The wicked ice chest was loaded with 5.71 kg of a solution of 25 g KHF_2 per 100 g H_2O. This quantity occupies a volume roughly equivalent to the 4.74 kg of water originally contained in the ice chest. Curve III presents the data obtained during this test run. As expected from the results of the Wicking Effect testing performed in a previous section, the heat sink capacitance fell far short of the desired results.

A 21 percent reduction in heat sink capacity was experienced. This is almost equivalent to the reduction in water content (there is 16 percent by weight less water in an equal volume of solution) and would, therefore, be equivalent to the water heat of fusion with little salt going into solution. It was postaulted that the ice chest wicking was retarding diffusion in the ice cavity and, therefore, redissolving of the salt.

After mutual agreement between Hamilton Standard and NASA, the wick testing was terminated and the ice chest was rebuilt with the wicks omitted. The expansion compensation modules were retained.

UNWICKED KHF_2/H_2O SOLUTION

The unwicked ice chest was loaded with 6.42 kg of a solution of 25 g KHF_2 per 100 g H_2O. The additional capacity results from the removal of the wick material. Curve IV presents this data. Again, little salt redissolved during the melt portion of the run with the gain nearly equivalent to the increased water charge.

UNWICKED SOLUTION WITH AGITATION

The run shown in Curve V was accomplished with a pneumatic shaker attached to the ice chest. The intent was to provide

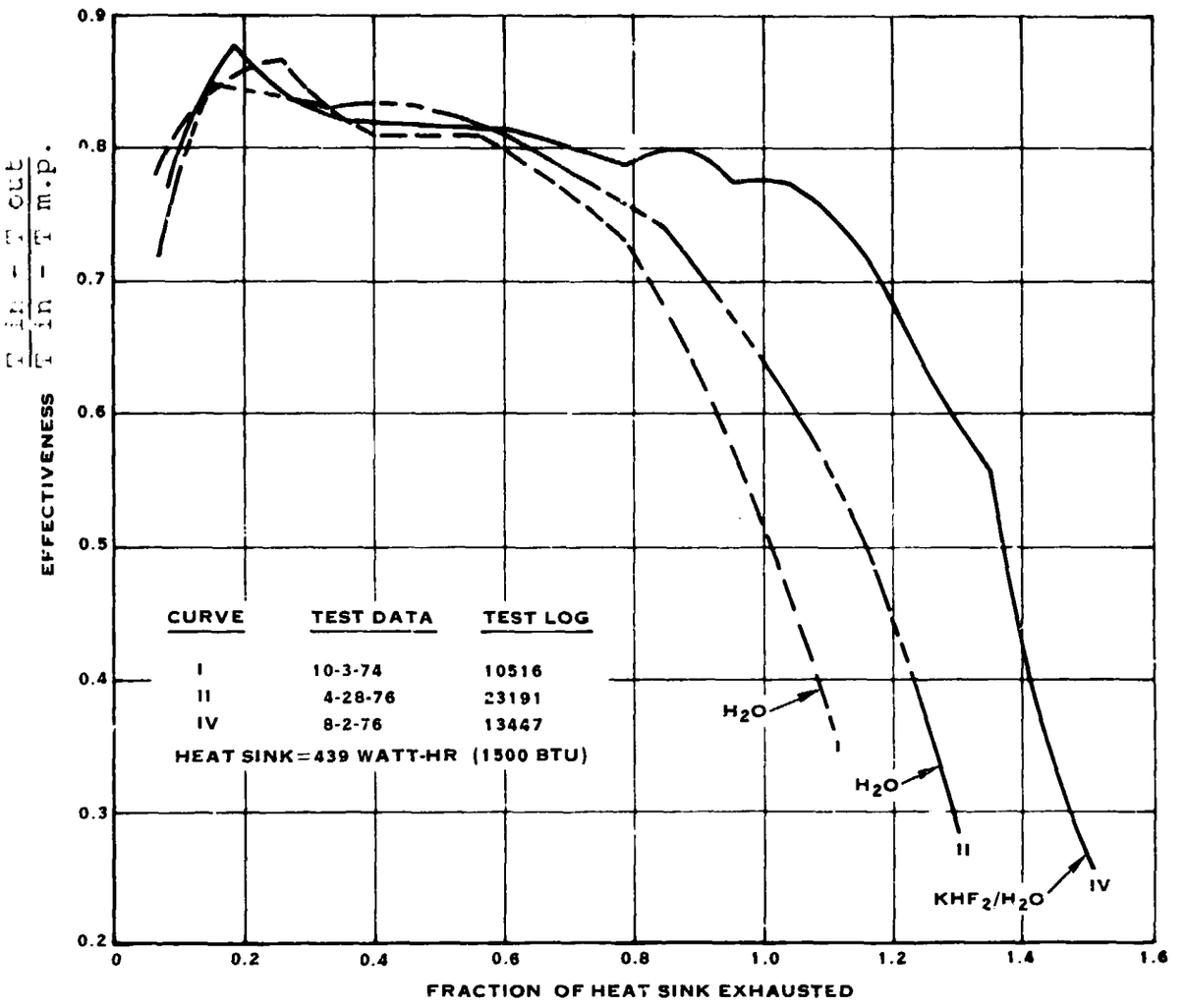

FIGURE 14. ICE CHEST PERFORMANCE

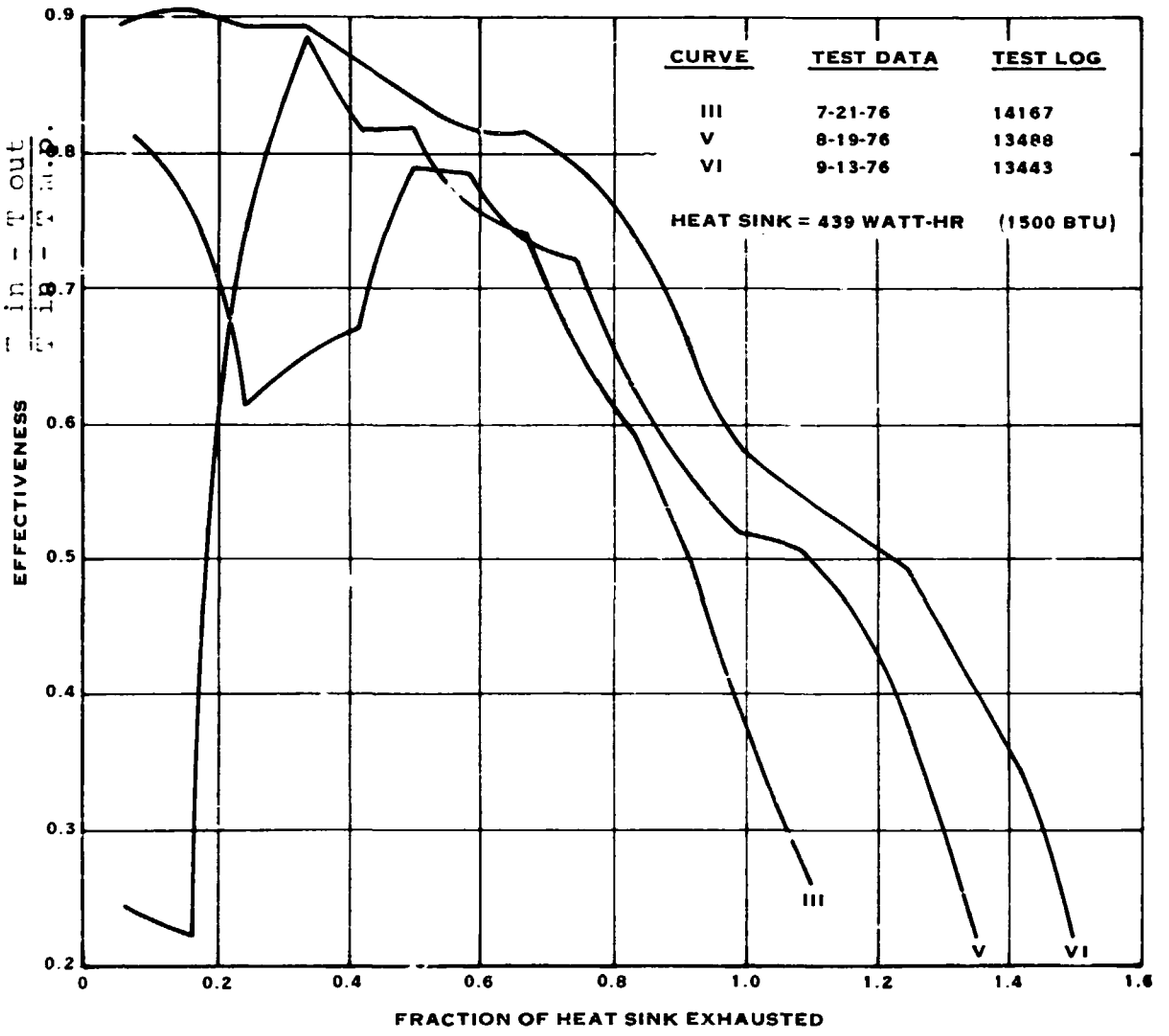

FIGURE 15. ICE CHEST PERFORMANCE

agitation to aid the redissolving of the KHF_2 in the H_2O during the melting of the solution, thereby increasing heat capacity. An examination of the data shows no appreciable improvement in heat absorption capacity.

UNWICKED SOLUTION WITH HORIZONTAL WICK CAVITIES

The run represented by Curve VI was accomplished with the ice pack reoriented 90° such that the individual cavities in the ice chest were oriented horizontally rather than vertically as had been done in all of the previous testing. The intent was to produce a short path, approximately 0.5 cm, over which any precipitated and settled salt had to diffuse rather than the original 35.5 cm diffusion path. Prior to freezing the ice chest, it was throughly thawed, oriented horizontally, and agitated for 30 minutes to insure complete redissolving of the salt. An examination of the data shows no appreciable change from the previous data.

EVALUATION

The results obtained from this Heat Sink Capacitance testing indicate a heat absorption capability of the 20% KHF_2 solution that is considerably different from that expected based on the previous Concentration Optimization testing. An examination of the differences in the conduct of the testing points to two potential differences, the first of which is the rate of redissolution of the KHF_2 during thawing and the second is the rate of freeze of the solution. Both differences arise from the fact that the hardware used for these tests is considerably larger than the calorimeter bomb.
An attempt has been made in this test series to evaluate redissolution rate but one of the problems encountered in the interpretation of the ice chest data is that the effectiveness of ice chest to heat exchanger interface and the ice chest internal resistance contribute a thermal lag to the heat removal rate, forcing us to conclude that the ice chest configuration is not suitable for our test purposes.

As was mentioned earlier in this section, the condition of the precipitated salt in the ice has a significant effect on the subsequent heat absorption capability. If the salt precipitates in the hydrate form a significantly larger heat absorption capability results than if the salt comes out of hydration as it precipitates in the ice. This is true because the salt hydration process is exothermic.

Testing was continued during the following task using a calorimeter with integral mechanical agitation to attempt to isolate the heat absorption anomalies.

LARGE SAMPLE TESTING

The large sample testing task was performed to determine the effect of simple mechanical stirring on the rate of redissolution of KHF_2 in water during thawing, and to study the effect of the rate of freeze of the KHF_2 solution on the subsequent heat absorption capability.

The apparatus used was a Paar Adiabatic Calorimeter modified to permit stirring of the solution after fusion transition. Two bombs were utilized. The first was a Paar thick-walled stainless steel combustion bomb with a special cover designed to interface with the modified adiabatic calorimeter to produce the mechanical stirring. The second was the UTRC brass bomb manufactured for the concentration optimization testing described in a previous section. This calorimeter, shown in Figures 16 and 17, utilizes a calorimeter bucket that contains a quantity of fluid into which the calorimeter bomb is immersed. The thermal constants of the calorimeter, such as the calorimeter bucket material and mass, the bucket fluid material and mass, and the calorimeter bomb materials and mass, have been calculated and experimentally verified. Precise measurements are made to determine the starting temperature of the bucket and its fluid and the bomb and its contents. The experiment is conducted to the point where the temperature of the bucket, bucket fluid, calorimeter bomb, and bomb contents are at equal temperatures; the resulting heat absorption of the bomb contents can be calculated. Adiabatic conditions are insured by maintaining the temperature of the fluid in the calorimeter jacket and top plate at the same temperature as the bucket fluid. Control determinations using pure water showed that the stirring mechanism has no effect on the determination of the heat of fusion of water-ice.

Heat absorption measurements utilizing the modified Paar bomb containing a 20% KHF_2 solution prepared at Hamilton Standard (HSD) yielding results slightly lower than those obtained using pure water. The solution was frozen to - 20°C by means of a freezer set at approximately - 23°C, and thawed in the calorimeter bomb utilizing mechanical stirring. The frozen temperature was verified by a thermocouple imbedded in the frozen sample. The results of these runs, 327.4 J/g and 329.7 J/g, are considerably less than the average value of 525 J/g obtained at United Technologies Research Center (UTRC) during the concentration optimization testing described in a previous section. The sample was refrozen and examined prior to thawing, and the fact that the sample was fully frozen was verified.

In an attempt of resolve the discrepancy it was decided to have

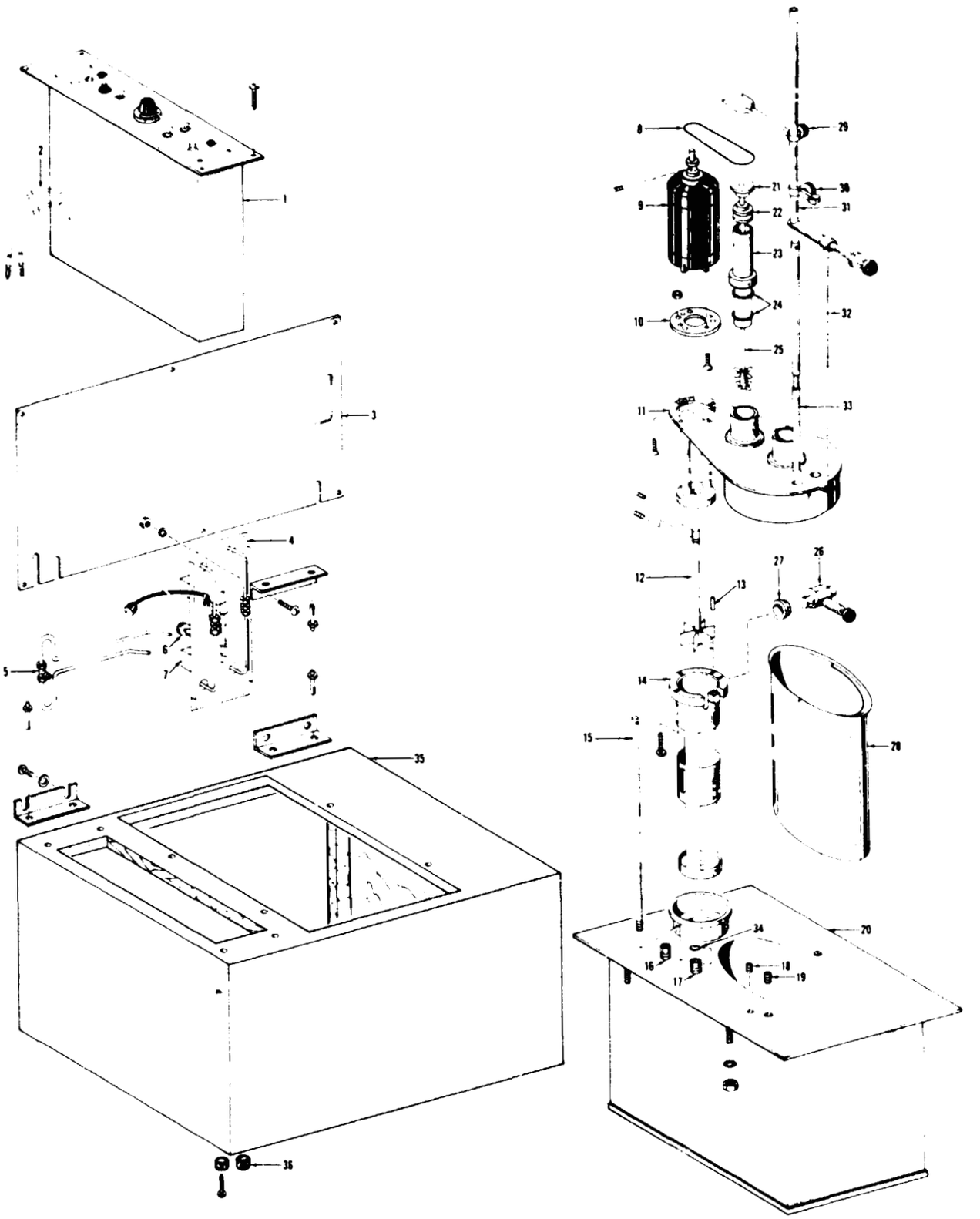

FIGURE 16. PÄAR ADIABATIC CALORIMETER CONFIGURATION

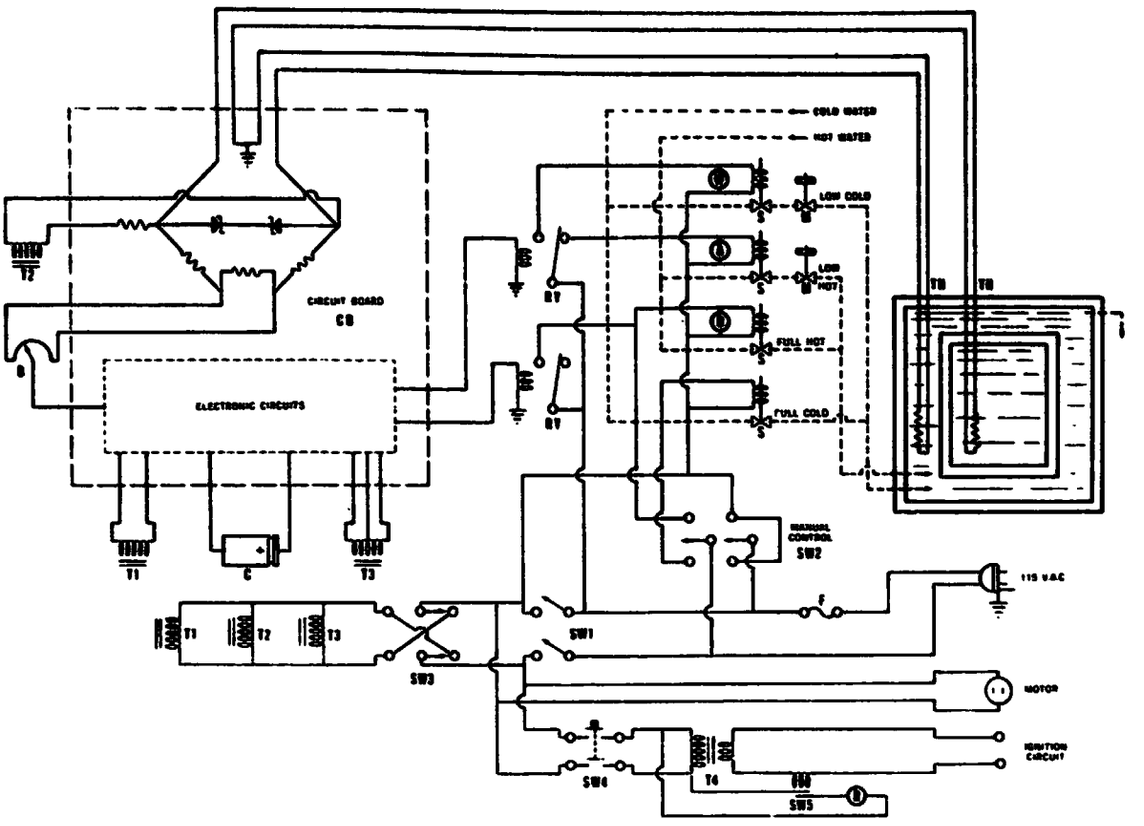

Schematic Wiring and Flow Diagram

Ref. No.	Part No.	Description
1	A300E	Control panel assembly for 1241 adiabatic calorimeter
2	A297E	Lead wire with banana plugs
3	371DD	Back panel
4	A403DD	Water control panel assby.
5	A368DD	Inlet tee
6	90HW	Metering valve
7	89HW	Solenoid valve
8	292DD	Belt
9	A162E	Calorimeter motor with cord
10	232DD	Motor mounting plate
11	A372DD	Calorimeter cover, bare
12	A227DD	Pump shaft with impeller
13	119VB	Pin
14	A402DD	Pump tube assembly
15	272DD	Thermometer support rod
16	A365DD	Thermistor fitting
17	A364DD	Thermometer fitting
18		3/8-24 x 3/8 soc hd screw
19	419DD	Plug
20	A376DD	Calorimeter jacket with top plate
21	251DD	Stirrer lift disc
22	239DD	Stirrer pulley
23	A355DD	Stirrer assembly with shaft, pulley and lift disc
24	417DD	Sealing ring
25	A237DD	Stirrer shaft with propellers
26	A323DD	Cover lift assembly
27	243DD2	Cover lift roller
28	A391DD	Calorimeter bucket
29	A332DD	Stirrer lift bracket
30	A270DD	Thermometer clamp
31	A358DD	Thermometer bracket with latch assembly
32	A359DD	Safety rod assembly
33	245DD	Therm. bracket support rod
34	422DD	Bumper ring
35	377DD	Calorimeter case, bare
36	80A2	Rubber foot
A	282E	Panel lamp assby., amber
	128E	Panel lamp bulb only
B	122E	Potentiometer, 500 ohm
	123E	Dial for potentiometer
C	269E	Capacitor, 500 mfd, 25 v.
CB	A253E	Circuit board assembly
F	139E	Fuse, 2 amp.
M	90HW	Metering valve, 1/8" NPT
R	126E	Panel lamp assby., red
RY	285E	Relay, plug-in type
S	89HW	Solenoid valve, 115 v.
SW1	101E	Switch DPST
SW2	129E	Switch DPDT
SW3	279E	Phase switch, DPDT
SW4	35E	Push switch, DPST
SW5	A276E	Magnetic switch assembly
T1	277E	Transformer, 12.6 v
T2	135E	Transformer, 6.3 v
T3	278E	Transformer, 25.2 v
T4	16E	Transformer, 21 v
TH	105E	Thermistor probe with plug
W	127E	Panel lamp assby., white

FIGURE 17. PAAR ADIABATIC CALORMETER SCHEMATIC AND PARTS LIST

UTRC load and test their brass bomb, and to test the same bomb and contents in the HSD calorimeter. The UTRC testing with a LN_2 frozen sample yielded a result of 580 J/g, somewhat larger than the average obtained during earlier UTRC testing. The same bomb and contents, LN_2 frozen and tested at HSD, yielded a result of 393.1 J/g which was far short of the UTRC value but represents the first time a value of heat absorption greater than that for water-ice had been measured at HSD. The bomb was dissassembled and the sample quantity was verified as was the thermal constant of the bomb.

The modified Paar thick walled stainless steel bomb was reloaded and frozen by LN_2 immersion. The freezing rate of this solution was slower than for the UTRC bomb due to the thermal lag caused by the thick stainless steel wall and the larger radial dimension of the sample. This test run yielded a heat absorption of 349.8 J/g, again higher than water-ice.

The UTRC brass bomb was frozen to - 20°C in the freezer, at a freeze rate faster than the original freeze rate of the Paar bomb due to the thin wall, high conductivity configuration of the UTRC brass bomb. This test run yielded a heat absorption of 409.7 J/g, the highest of the runs performed at Hamilton Standard. The test runs are tabulated in Table XXII. Testing was terminated at this point because the statement of work for this task specified six calorimeter runs and ten runs have been completed at this point.

The data obtained from this test series indicates that there is a real and measurable increase in the heat absorption of the KHF_2 solution compared to pure water when the solution is allowed to cool rapidly either by use of liquid nitrogen immersion or by use of the highly conductive UTRC brass bomb. The test method has been demonstrated by the H_2O runs to be accurate within +4 J/g so the inconsistencies measured must be assumed to exist, and the indication is that there is an unidentified factor involved in the liquid-solid phase transition of the KHF_2/H_2O solution.

Two approaches can be pursued to further quantify the effect of freezing rate on the heat absorption available during thaw. The first involves generating a liquid-solid phase diagram for the KHF_2/H_2O solution to aid in understanding the effect of freeze rate on the resulting chemical formations and, hence, the heat absorption capability of the material. This diagram is necessary to fully evaluate the potential of the solution for further applications. The second is to further modify the Paar adiabatic calorimeter bomb to minimize bomb mass and thermal mass, and to design a controlled freezing rate device to experimentally develop and verify heat absorption parameters associated with the freeze rate of the potassium bifluoride/water solution:

TABLE XXII

HEAT ABSORPTION TEST RESULTS

MATERIAL	BOMB	COOLING CONDITIONS	TEST SITE	AGITATION	\H(J/g)
H_2O	Paar	Freezer (-23°C)	HSD	Yes	334.7
H_2O	Paar	Freezer (-23°C)	HSD	No	336.0
H_2O	Paar	Freezer (-23°C)	HSD	Yes	330.6
H_2O	UTRC	Freezer (-23°C)	HSD	No	331.1
KHF_2/H_2O	Paar	Freezer (-23°C)	HSD	Yes	327.4
KHF_2/H_2O	Paar	Freezer (-23°)	HSD	Yes	329.7
KHF_2/H_2O	UTRC	LN_2 (-195°C)	UTRC	No	580
KHF_2/H_20	UTRC	LN_2 (-195°C)	HSD	No	393.1
KHF_2/H_20	Paar	LN_2 (-195°C)	HSD	Yes	349.8
KHF_2/H_20	UTRC	Freezer (-23°C)	HSD	No	409.7

SOLUTION PROPERTIES SUMMARY

Table XXIII contains a summary of properties for the optimum concentration solution consistency of 25g KHF_2/100 g H_2O and for the slurry solution consistency of 90% by volume of the 25g KHF_2/100g H_2O solution and 10% by volume of ethanol.

TABLE XXIII

KHF_2 SOLUTION PROPERTIES SUMMARY

Optimum Concentration Solution: 25g KHF_2/100g H_2O

Slurry Solution: 90% by volume 25g KHF_2/100g H_2O
10% by volume ethanol

Compatible Metals: Inconel 625, Hastelloy C, AISI 347, or any combination of these metals

Thermal Capacity During Thaw:

Optimum Concentration, Small Sample	525 J/g
Optimum Concentration, Large Sample	Highly dependent on freeze rate
Slurry, Small Sample	467 J/g
Slurry, Large Sample	Highly dependent on freeze rate

Thermal Conductivity:

Optimum Concentration, Liquid	0.535 W/m °C
Optimum Concentration, Solid	2.31 W/m °C
Slurry, Liquid	0.454 W/m °C
Slurry, Solid	0.989 W/m °C

Thermal Expansion:

Optimum Concentration, Liquid	1.74×10^{-4} cm^3/cm^3°C from 3°C to 25°C
Optimum Concentration, Solid	1.02×10^{-4} cm^3/cm^3°C from -14.8°C to -31.5°C
Optimum Concentration, Liquid/ Solid Transition	0.095 cm^3/cm^3
Slurry	Refer to Figure 12

APPENDIX A

CONFIGURATION VERIFICATION TEST PLAN

HAMILTON STANDARD

SVHSER 7163
C44-202

PROTOTYPE ICE PACK HEAT SINK SUBSYSTEM
CONFIGURATION VERIFICATION TEST PLAN

PREPARED UNDER CONTRACT NAS 2-8665

BY

HAMILTON STANDARD
DIVISION OF UNITED TECHNOLOGIES CORPORATION
WINDSOR LOCKS, CONNECTICUT

FOR

NATIONAL AERONAUTICS AND SPACE ADMINISTRATION
AMES RESEARCH CENTER
MOFFETT FIELD, CALIFORNIA

APRIL 1976

Prepared by: _____
G. Roebelen
Program Engineer

Approved by: _____
D. Lizdas
Program Manager

TABLE OF CONTENTS

1.0 SCOPE

This plan of test defines the test program to be performed by Hamilton Standard on the Ice Pack Heat Sink Subsystem hardware fabricated and delivered to NASA Ames Research Center under Contract NAS 2-7011, Phase II. The test program is intended as a means for comparing the heat absorption capability of an Ice Chest (freeze/thaw mode) containing distilled water with the heat absorption capability of the same Ice Chest (freeze/thaw mode) containing a mixture of potassium bifluoride and distilled water.

2.0 TEST SEQUENCE

The performance test program consists of the following tests performed in the sequence defined:

1. Evaluation of ice chest freeze/thaw performance utilizing distilled water as the heat absorption chemical.

2. Evaluation of ice chest freeze/thaw performance utilizing a mixture of potassium bifluoride (KHF_2) and distilled water as the heat absorption chemical.

Deviation from the test sequence or test procedure requires approval of the cognizant program engineer.

3.0 TEST ENVIRONMENT

The test environment for all portions of this test will be vacuum.

4.0 TEST EQUIPMENT

All portions of this test program will be performed in the Hamilton Standard Space Systems Department Space Laboratory. Except for the Rig 25 vacuum facility, portable equipment compatible with the test unit and the test requirements as defined by this plan of test will be utilized.

5.0 DEFINITION OF TESTS

5.1 Evaluation of Ice Chest Freeze/Thaw Performance Utilizing Distilled Water as the Heat Absorption Chemical

5.1.1 Instrumentation and Equipment

Qty	Item	Range	Accuracy
1	DC Power Supply	0-30 VDC @ 3 ampere	± 0.1 volt
1	DC Voltmeter	0-30 VDC	± 0.05 volt
1	DC Ammeter	0-30 ampere	± 0.05 ampere
1	AC Voltmeter	0-120 VAC	± 1.0 volt
1	AC Ammeter	0-10 amp	± 1.0 ampere
1	Flowmeter	0-0.1 gpm	± 0.005 gpm
1	Flowmeter	0-0.425 gpm	± 0.025 gpm
1	Flowmeter	0-0.58 gpm	± 0.025 gpm
4	Pressure Gauge	0-30 psia	± 0.05 psi
1	Coolant Pump	0.48-0.53 gpm	± 0.02 gpm
1	Heat Load	0-2000 Btu/hr	± 20 Btu/hr
1	L&N Thermocouple Readout	0-100°F	± 0.4°F
4	Thermocouple	0-100°F	± 0.1°F

5.1.2 Test Set-Up

This test is performed on Rig 25 in the Space Systems Department Space Laboratory. Figure 1 schematically illustrates the test set-up.

5.1.3 Test Procedure

a. Install the ice pack heat exchanger assembly in the vacuum chamber of Rig 25 and plumb the hardware and wiring per Figure 1.

b. Set the power supply to 27 vdc and start the pump/motor. Close the bypass flow valve. Open the flowmeter bypass valve. Open the heat exchanger flow valve. Fill system with water through water fill port. Bleed air from system utilizing water fill port valve and air bleed vent valve and pressurize pump inlet to 5 psig. Adjust the heat exchanger flow valve to obtain a system flow of 0.5 gpm.

c. Check thermocouples T_1, T_2, T_3, T_4.

d. Switch the bladder control valve to vacuum.

e. Chill the system to 45°F using an external cooling pack applied to heat exchanger.

f. Install an insulated frozen distilled water ice chest on the heat exchanger assembly. Close the vacuum chamber and evacuate to 10^{-4} mmHg (0.1 micron).

5.1.3 Test Procedure (Continued)

g. Adjust the heater control to apply 2000 Btu/hr (587 volt amperes) to the LCG simulator.

h. When the outlet temperature of the LCG simulator reaches 58°F, pressurize the bladder to 20 psia.

i. Adjust the heat exchanger flow valve and bypass flow valve to maintain the heat exchanger outlet temperature at 50°F and the system flow at 0.5 gpm. When the bypass flow reaches zero, continue running until the heat exchanger outlet temperature reaches 65°F. Shut off the heater and the pump/motor. Repressurize the chamber and remove the ice chest. Refreeze the ice chest.

j. Repeat b, c, d, and f.

k. Adjust the heater control to apply 1500 Btu/hr (440 volt-amperes) to the LCG simulator.

l. When the outlet temperature of the LCG simulation reaches 76°F, pressurize the bladder to 20 psia.

m. Adjust the heat exchanger flow valve and bypass flow valve to maintain the heat exchanger outlet temperature at 70°F and the system flow at 0.5 gpm. When the bypass flow reaches zero, continue running until the heat exchanger outlet temperature reaches 80°F. Shut off the heater and the pump/motor. Repressurize the chamber and remove the ice chest. Refreeze the ice chest.

n. Repeat j, k, l, and m, except adjust heater control to 750 Btu/hr (220 volt-amperes) and pressurize the bladder when the outlet temperature of the LCG simulator reaches 88°F. Adjust valves to maintain the heat exchanger outlet temperature at 85°F and shut down when the heat exchanger outlet temperature reaches 90°F.

5.1.4 Test Requirements

Each of the tests must be run until the heat exchanger outlet temperature cannot be maintained at the specified temperature. For each run record the following condition vs. time:

1. Heater voltage
2. Heater amperage
3. System flow
4. Heat exchanger flow
5. Pump inlet pressure
6. Bladder pressure
7. Heat exchanger inlet pressure
8. Heat exchanger outlet pressure
9. Heat exchanger inlet temperature
10. Heat exchanger outlet temperature
11. LCG inlet temperature
12. LCG outlet temperature
13. Vacuum chamber pressure

5.2 Evaluation of Ice Chest Freeze/Thaw Performance Utilizing a Mixture of Potassium Bifluoride (KHF2) and Distilled Water as the Heat Absorption Chemical

5.2.1 Instrumentation and Equipment

Qty	Item	Range	Accuracy
1	DC Power Supply	0-30 VDC @ 3 ampere	± 0.1 volt
1	DC Voltmeter	0-30 VDC	± 0.05 volt
1	DC Ammeter	0-3 ampere	± 0.05 ampere
1	AC Voltmeter	0-120 VAC	± 1.0 volt
1	AC Ammeter	0-10 amp	± 0.1 ampere
1	Flowmeter	0-0.1 gpm	± 0.005 gpm
1	Flowmeter	0-0.425 gpm	± 0.025 gpm
1	Flowmeter	0-0.58 gpm	± 0.025 gpm
4	Pressure Gauge	0-30 psia	± 0.05 psi
1	Coolant Pump	0.48-0.53 gpm	± 0.02 gpm
1	Heat Load	0-2000 Btu/hr	± 20 Btu/hr
1	L&N Thermocouple Readout	0-100°F	± 0.4°F
4	Thermocouple	0-100°F	± 0.1°F

5.2.2 Test Set-up

This test is performed on Rig 25 in the Space Systems Department Space Laboratory. Figure 1 schematically illustrates the test set-up.

5.2.3 Test Procedure

a. Install the ice pack heat exchanger assembly in the vacuum chamber of Rig 25 and pumb the hardware and wiring per Figure 1.

b. Set the power supply to 27 vdc and start the pump/motor. Close the bypass flow valve. Open the flowmeter bypass valve. Open the heat exchanger flow valve. Fill system with water through water fill port. Bleed air from system utilizing water fill port valve and air bleed vent valve and pressurize pump inlet to 5 psig. Adjust the heat exchanger flow valve to obtain a system flow of 0.5 gpm.

c. Check thermocouples T_1, T_2, T_3, T_4.

d. Switch the bladder control valve to vacuum.

e. Chill the system to 45°F using an external cooling pack applied to heat exchanger.

f. Install an insulated frozen potassium bifluoride-distilled water ice chest on the heat exchanger assembly. Close the vacuum chamber and evacuate to 10^{-4} mmHg (0.1 micron).

g. Adjust the heater control to apply 2000 Btu/hr (587 volt-amperes) to the LCG simulator.

h. When the outlet temperature of the LCG simulator reaches 58°F, pressurize the bladder to 20 psia.

i. Adjust the heat exchanger flow valve and bypass flow valve to maintain the heat exchanger outlet temperature at 50°F and the system flow at 0.5 gpm. When the bypass flow reaches zero, continue running until the heat exchanger outlet temperature reaches 65°F. Shut off the heater and the pump/motor. Repressurize the chamber and remove the ice chest. Refreeze the ice chest.

j. Repeat b, c, d, and f.

k. Adjust the heater control to apply 1500 Btu/hr (440 volt-amperes) to the LCG simulator.

5.2.3 Test Procedure (Continued)

l. When the outlet temperature of the LCG simulation reaches 76°F, pressurize the bladder to 20 psia.

m. Adjust the heat exchanger flow valve and bypass flow valve to maintain the heat exchanger outlet temperature at 70°F and the system flow at 0.5 gpm. When the bypass flow reaches zero, continue running until the heat exchanger outlet temperature reaches 80°F. Shut off the heater and the pump/motor. Repressurize the chamber and remove the ice chest. Refreeze the ice chest.

n. Repeat j, k, l, and m, except adjust heater control to 750 Btu/hr (220 volt-amperes) and pressurize the bladder when the outlet temperature of the LCG simulator reaches 88°F. Adjust valves to maintain the heat exchanger outlet temperature at 85°F and shut down when the heat exchanger outlet temperature reaches 90°F.

5.2.4 Test Requirements

Each of the tests must be run until the heat exchanger outlet temperature cannot be maintained at the specified temperature. For each run, record the following condition vs. time:

1. Heater voltage
2. Heater amperage
3. System flow
4. Heat exchanger flow
5. Pump inlet pressure
6. Bladder pressure
7. Heat exchanger inlet pressure
8. Heat exchanger outlet pressure
9. Heat exchanger inlet temperature
10. Heat exchanger outlet temperature
11. LCG inlet temperature
12. LCG outlet temperature
13. Vacuum chamber pressure

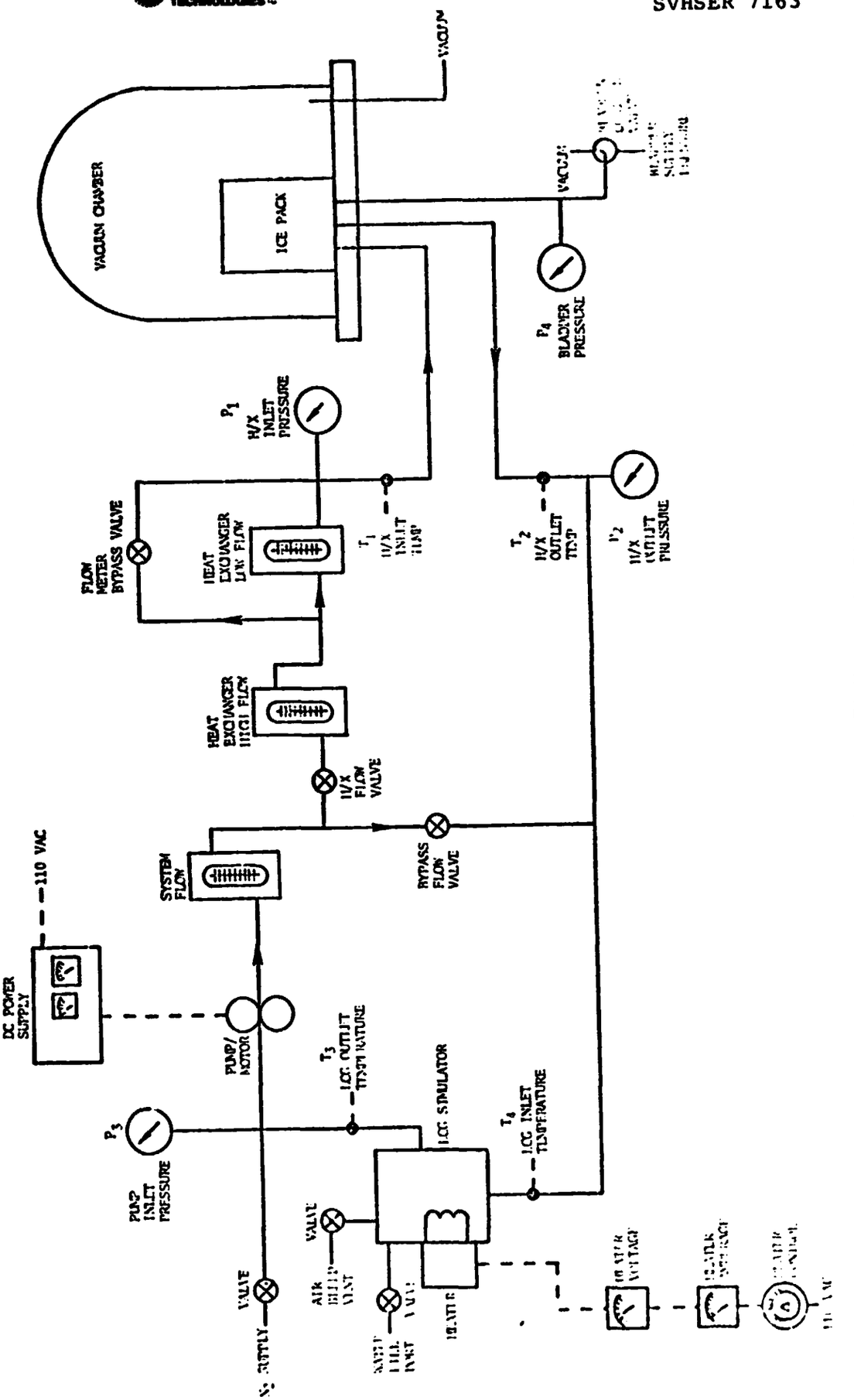

FIGURE 1 CONFIGURATION VERIFICATION TEST SET-UP

Hamilton Standard DIVISION OF UNITED AIRCRAFT CORPORATION
WINDSOR LOCKS, CONNECTICUT 06096

SPACE & LIFE SYSTEMS LABORATORY

LOG OF TEST

TYPE OF TEST: ICE PACK ICE CHEST
TEST ENGINEER:
NAME OF RIG: # 25
PROJECT & ENG. ORDER NO.: NAS 2 - 8665

SHEET ___ OF ___ DATE ___
TEST PLAN NO
MODEL NO
PART NO.
SERIAL NO
OPERATORS

TIME	TEST TIME	VOLTS	AMPS	AMPS	WATTS		SYST	HX	HX	HX IN	HX OUT		HX IN	HX OUT	ΔT 27-28	LCG IN	LCG OUT		WALL TEMP	[illegible] PRESS		[illegible]
		AC	AC	AC			%	%	%	PSIA	PSIA		°F27	°F28	MV	°F1	°F2		°F29	PSIA		[illegible]

REMARKS:

23189

APPENDIX B

TEST LOG SHEETS

Hamilton Standard DIVISION OF UNITED AIRCRAFT CORPORATION
WINDSOR LOCKS, CONNECTICUT 06096

SPACE & LIFE SYSTEMS LABORATORY

LOG OF TEST

TYPE OF TEST: ICE PACK - ICE CHEST (H2O)
TEST ENGINEER: R. PETILLO
NAME OF RIG: #25
PROJECT & ENG. ORDER NO.: NAS2-8665

SHEET 1 OF 2, DATE 4/28/76
TEST PLAN NO.
MODEL NO.
PART NO.
SERIAL NO.
OPERATORS: E. LASZCZYK

TIME	TEST TIME	VOLTS	AMPS	AMPS	WATTS	SYST	SYST	HX	HX	HX IN	HX OUT	FLOW HX	HX IN	HX OUT	ΔT 27-28	LCG IN	LCG OUT	Q	WALL TEMP	BLADDER PRESS	Q	CHAMB PRESS
		AC	AC	AC		GPM	%	%	%	PSIA	PSIA	GPM	°F27	°F28	MV	°F1	°F2	[illegible]	°F29	PSIA		TORR
1036		76	3.55	1.93	441	0.5	52.5	53	[illegible]	17.5	15.3	.60	73.0	72.5	.046	73	75.5	[illegible]	64.5	0		1X10-4
[illegible]	START 3	76	3.56	1.94	440	↓	52.5	26.5	.121	16.25	15.25	.30	76.0	45.0	.680	70	76	439	64.5	20	[illegible]	2.6X10-4
[illegible]	8	76	3.57	1.95	442		52.5	17.5	[illegible]	15.9	15.25	.19	74.0	38.5	.778	70	75	36.0	64.5	20	[illegible]	5.0X10-4
1050	13	76	3.56	1.95	441		52.5	17.5	[illegible]	16.0	15.25	.22	75.5	39.0	.792	70	75.5	403	65.0	20	[illegible]	5.3X10-4
1055	18	76	3.87	1.95	442		52.5	19.	[illegible]	15.95	15.25	.21	75.0	39.4	.785	70	75.	[illegible]	65.5	20	[illegible]	5.7X10-4
1100	23	76	3.56	1.95	441		52.5	18.5	[illegible]	15.95	15.25	.20	75.0	39.2	.786	70	75.5	[illegible]	65.0	20	[illegible]	5.5X10-4
1105	28	76	3.56	1.94	440		52.5	18.5		15.95	15.25	.20	75.0	39.5	.784	70	75.5	[illegible]	65.0	20	[illegible]	5.4X10-4
1110	33	76	3.57	1.95	442		52.5	19	[illegible]	15.95	15.25	.21	75.0	40.0	.776	70	76	[illegible]	65.0	20	[illegible]	5.1X10-4
1115	38	76	3.57	1.95	442		52.5	19.5	[illegible]	15.95	15.25	.22	75.0	41.0	.765	70	76	↓	65.5	20	[illegible]	4.8X10-4
1120	43	76	3.57	1.95	442		52.5	20	[illegible]	16.0	15.25	.22	75.0	43.0	.744	70	76		65.5	20	[illegible]	3.6X10-4
1125	48	76	3.56	1.95	441		52.5	20.5	[illegible]	16.0	15.25	.23	75.0	43.1	.722	70	76.5	[illegible]	65.5	20	[illegible]	3.1X10-4
1130	53	76	3.56	1.95	441		52.5	22.		16.05	15.25	.25	75.5	45.4	.679	70	76.5		65.5	20	[illegible]	2.4X10-4
1135	58	76	3.56	1.95	441		52.5	23	[illegible]	16.1	15.25	.26	75.5	47.8	.627	70	76	429	65.5	20	[illegible]	1.6X10-4
1140	63	76	3.56	1.95	441		52.5	26	[illegible]	16.2	15.25	.29	75.5	51.0	.561	70	76		65.5	20	[illegible]	8X10-4
1145	68	76	3.56	1.95	441		52.5	33.5		16.45	15.25	.38	75.5	55.0	.474	70	76		65.5	20	[illegible]	7X10-5
1150	73	76	3.56	1.95	441		52.5	40.5	.181	16.9	15.25	.46	75.0	59.4	.371	70	76		65.5	20	[illegible]	5.7X10-5
1155	78	76	3.56	1.95	441		52.5	58	[illegible]	17.9	15.20	.66	76.0	65.0	.252	70	76		66.0	20	[illegible]	4.7X10-5
1200	83	76	3.55	1.95	440		52.5	100+	[illegible]	23.8	15.25	1.1+	76.0	71.0	.122	70	76	✓	66.0	20	[illegible]	4.3X10-5
1205	88	76	3.55	1.95	440	↓	52.5	100+		23.8	15.25	1.1+	77.5	73.7	.096	73	78	[illegible]	66.0	20		4.2X10-5
1210	93	76	3.65	1.95	440	0.5	52.5	100+		23.8	15.25	1.1+	80.5	77.1	.088	76	80.5	[illegible]	66.0	20		4.1X10-5

REMARKS:

WT OF WATER IN CHEST 11.21 LBS

ICE CHEST INSTALL. 4 MIN.
TEMP -20°C

$GPM(\ldots)(60) = GPM(T_2 - T_1)(1.46\ldots)$

REPRODUCIBILITY OF THE ORIGINAL PAGE IS POOR

23191

SVHSER 7163

Hamilton Standard DIVISION OF UNITED AIRCRAFT CORPORATION
WINDSOR LOCKS, CONNECTICUT 06096

SPACE & LIFE SYSTEMS LABORATORY

LOG OF TEST

TYPE OF TEST: ICE PACK ICE CHEST (11.0)
TEST ENGINEER: R. PETILLO
NAME OF RIG: #25
PROJECT & ENG. ORDER NO.: NAS 2 · 8665

SHEET 2 OF 2 DATE 4/28/76
TEST PLAN NO.
MODEL NO.
PART NO.
SERIAL NO.
OPERATORS: E. LASZCZYK/G. HOWE

TIME	TEST TIME	VOLTS	AMPS	AMPS	WATTS	SYST	SYST	HX	HX	HX IN	HX OUT	FLOW HX	HX IN	HX OUT	ΔT 27-28	LCG IN	LCG OUT	WALL TEMP	[illegible]	BLADDER PRES		CHAMB PRES
		AC	AC	AC		GPM	%	%	%	PSIA	PSIA	GPM	$°F_{27}$	$°F_{28}$	MV	$°F_1$	$°F_2$	$°F_{29}$	[illegible]	PSIA		TORR
[illegible]	78	76	3.55	1.95	440	.5	83.5	100+		23.7	15.25	1.1+	83.0	80.0	.080	79	53.5	66.0	330	20		4X10
[illegible]	100	76	3.55	1.75	440	.5	83.5	100+		23.7	15.25	1.1+	84.5	81.5	.079	80	54.5	66.0	[illegible]	20		4X10

REMARKS:

SVHSER 7163

23193

HSP-179 1A 1/66

Hamilton Standard DIVISION OF UNITED AIRCRAFT CORPORATION
WINDSOR LOCKS, CONNECTICUT 06096

SPACE & LIFE SYSTEMS LABORATORY

LOG OF TEST

TYPE OF TEST: Ice Pack KHF_2 / H_2O

TEST ENGINEER: Unwicked w/ Paper Between

NAME OF RIG: 1500 BTU/HR

PROJECT & ENG. ORDER NO.

SHEET 1 OF 2 DATE 8/2/76

TEST PLAN NO.

MODEL NO.

PART NO.

SERIAL NO.

OPERATORS

Time	Test Time	Volts	Amp	Amp	Watt	Flo Syst	Syst	Hx	Hx	Hx In	Hx Out	Flow Hx	Hx In	Hx Out	ΔT	LCG In	LCG Out	Wall Temp		Blad Press		Chamb Press
	Min	AC	AC	AC		GPM	%	%	%	PSIA	PSIA	GPM	°F	°F	MV	°F	°F	°F		PSIG		μ
													59.5	59.5		60	60					
925	Start	76	1.9	3.9			82.5	Fill	~~[illegible]~~	2445	15.0	.1	75.0	62.0	.426	68.0	75.0	—		7		
930	5	76	1.9	3.9			82.5		14.0	—	—	.1	72.0	41.0	.780	66.0	71.0					
935	10	76	1.9	3.9			82.5		14.7	—	—	.1	73.0	37.0	.7675	65.5	72.5					
940	15	76	1.9	3.9			825		19.75	-	-	.1	71.5	36.5	.720	65.0	71.0					
45	20	76	1.9	3.9			82.5		14.75	—	—	.1	71.0	39.0	.700	64.0	70.0				.82	
50	25	76	1.9	3.9			82.5		14.75			.1	70.5	39.0	.6875	64.0	70.0				.78	
55	30	76	1.9	3.9			82.5		14.75			.1	70.0	39.0	.6825	64.0	70.0					
1000	35	76	1.9	3.9			82.5		14.75			.1	69.5	39.0	.675	63.5	69.5					
05	40	76	1.9	3.9			82.5		14.60			.1	69.5	39.5	.665	63.5	69.5				.8	
10	45	76	1.9	3.9			82.5		14.5				69.5	40.0	.665	64.0	70.0					
15	50	76	1.9	3.9			82.5		19.5				69.5	39.5	.6525	64.0	70.0				.8	
20	55	76	1.9	3.9			82.5		14.5				69.5	40.5	.645	64.0	70.5					
25	60	76	1.9	3.9			82.5		14.5				70.0	40.5	.645	64.0	70.0					
30	65	76	1.9	3.9			825		14.7				71.0	42.0	.620	65.0	71.0					
35	70	76	1.9	3.9			82.5		15.0				71.0	44.0	.59	65.5	70.5				.692	
40	75	76.	1.9	3.9			82.5		15.5			.11	72.5	47.5	.5525	66.0	72.0					
45	80	76	1.9	3.9			82.5		27.5			.13	72.5	50.0	.475	66.5	72.5					
50	85	76	1.9	3.9			82.5		35.0			.16	72.5	57.0	.370	66.0	72.0					
55	90	76	1.9	3.9			82.5		55.0			.24	72.5	61.5	.240	65.5	71.5					
1100	95	76	1.9	3.4			82.5		67.0			.3	72.5	64.0	.190	66.0	72.0					

SVHSER 7163

REMARKS:

Ice chest −18°C

• Switched Flowmeters

14.15 LBS 25 g KHF_2 / 100 g H_2O solution

13447

NSP-175 1A 1/66

Hamilton Standard DIVISION OF UNITED AIRCRAFT CORPORATION
WINDSOR LOCKS, CONNECTICUT 06096

SPACE & LIFE SYSTEMS LABORATORY

LOG OF TEST

TYPE OF TEST: ICE PACK - ICE CHEST (KHF_2)
TEST ENGINEER: R. PETILLO (WICKED)
NAME OF RIG: #25
PROJECT & ENG. ORDER NO.: NAS 2 - 8665

SHEET 1 OF 1 DATE 7/24/76
TEST PLAN NO.
MODEL NO.
PART NO.
SERIAL NO.
OPERATORS

TIME	TEST TIME	VOLTS	AMPS	AMPS	WATTS	FLOW SYST	SYST	HX	Hx	HX IN	HX OUT	FLOW HX	HX IN	HX OUT	ΔT 27-28	LCG IN	LCG OUT	WALL TEMP		GAP PRESS		CHEM PRESS
	MIN	AC	AC	AC		GPM	%	%	%	PSIA	PSIA	GPM	°F 27	°F 28	MV	°F 1	°F 2	°F 29		PSID		MILLIB
2045	—	0	0	0	0	.5	82.5	—								—	68.0			0		—
2135	50 TARE	76	3.82	1.88	428.2			—	65	17.8	15.3	0.288	80	66	.338	—	76.0	67		20		260
2140	5	76	3.87	1.89	439.3			—	100	21.5	15.2	0.436	77	66	.242	66.2	73.0	67				230
2145	10	76	3.89	1.89	439.3			—	100	22.0	15.0	0.434	72.5	63.5	.215	68.3	71.0	67				
2150	15	76	3.92	1.91	443.1			—	10	15.3	15.0	0.053	76.5	42	.534	69.5	71.9	67				
2155	20	76	3.90	1.90	440.8			—	17	15.6	15.1	0.08	75.5	37	.861	70.0	75.2	67				195
2200	25	76	3.90	1.90	440.8			—	18	15.6	15.2	0.082	75.5	40	.800	70.0	75.9	67				
2205	30	76	3.90	1.90	440.8			—	18	15.6	15.2	0.082	76	40	.800	70.0	76.0	67				
2210	35	76	3.89	1.90	440.0			—	20	15.7	15.2*	0.094	76	42.5	.767	70.0	76.0	67				170
2215	40	76	3.90	1.90	440.8			—	21	16.7	15.25	0.099	76.5	43.5	.735	70.0	76.0	66				
2220	45	76	3.90	1.91	441.6			—	23	16.8	15.3	0.106	76.5	47.5	.666	70.0	76.2	66				
2225	50	76	3.90	1.90	440.8			—	27	15.9	15.3	0.124	77	52.5	.602	70.0	76.3	66				145
2230	55	76	3.90	1.91	441.6			—	29	16.0	15.3	0.133	77	54.5	.525	70.0	76.2	66				
2235	60	76	3.90	1.91	441.6			—	37	16.4	15.3	0.168	76.5	58.5	.400	70.0	76.2	66.5				
2240	65	76	3.89	1.90	440.0			—	51	17.1	15.3	0.228	77	65	.286	70.0	76.2	66.5				128
2245	70	76	3.90	1.90	440.8			—	96	20.9	15.15	0.420	77	71	.168	70.0	76.1	66				
2250	75	76	3.90	1.90	440.8			—	105*	23.4	15.0	0.456*	78	72.5	.108	72.1	77.2	66				115
2255	80	76	3.90	1.90	440.8			—		23.3	15.0		80	76	.100	74.2	79.8	66.5				
2300	85	76	3.90	1.90	440.8			—		23.3	14.95		82.5	79	.082	76.8	82.0	66.5				
2305	90	76	3.90	1.90	440.8			—		23.3	14.95		85	91.5	.087	79.2	84.9	66				
2310	95	76	3.90	1.90	440.8	.5	82.5	—	100*	23.3	14.95	0.436*	87.5	84	.091	81.5	87.0	66		20		92

REMARKS

INITIAL TEMP OF ICE CHEST -21 °C E.O.T.
TIME TO INSTALL 3 MIN.
12.59 LBS 25g KHF_2/100g H_2O SOLUTION

8YHSER 7163

14167

HSF-175 1A 1/66

Hamilton Standard DIVISION OF UNITED AIRCRAFT CORPORATION
WINDSOR LOCKS, CONNECTICUT 06096

SPACE & LIFE SYSTEMS LABORATORY
LOG OF TEST

TYPE OF TEST: Ice Pack
TEST ENGINEER:
NAME OF RIG:
PROJECT & ENG. ORDER NO.

SHEET 2 OF 2 DATE 8/2/76
TEST PLAN NO.
MODEL NO.
PART NO.
SERIAL NO.
OPERATORS

Time	Test Time	Volts	Amp	Amp	Watt	Flo Syst	Syst	Hx	Hx	Hx In	Hx Out	Flow Hx	Hx In (27)	Hx Out (28)	ΔT	Leg In	Leg Out	Wall Temp		Blad	Σ	Chamb
	Min	AC	AC	AC		GPM	%	%	%	PSIA	PSIA	GPM	°F	°F								
1105	100	95 76	1.9	3.9			82.5		Full			.5	74.0	68.5		67	73		[illegible]		[illegible]	
10	105	95 76	1.9	3.9			82.5		Full				75.0	71.0	.0975	68.5	74.5		[illegible]		[illegible]	
15	110	95 76	1.9	3.9			82.5		Full				78.0	74.0	.0925	71.0	76.5		[illegible]		[illegible]	
20	115	95 76	1.9	3.9			82.5		Full				79.0	76.0	.0875	73.0	79.0		[illegible]			
25	120	95 76	1.9	3.9			82.5		Full				81.5	78.5	.0880	75	81.0		[illegible]			
30	125	95 76	1.9	3.9			82.5		Full				84.0	80.0	.0825	77	83.0		[illegible]			
35	130	76	1.9	3.9			82.5		Full				87.0	84.0	.0750	80	86.0					
40	135	76	1.9	3.9			82.5		Full				88	85.5	.0750	81	87					
													EOT									

REMARKS:

13448

HSF-175 1A 1/66

Hamilton Standard DIVISION OF UNITED AIRCRAFT CORPORATION
WINDSOR LOCKS, CONNECTICUT 06096

SPACE & LIFE SYSTEMS LABORATORY

LOG OF TEST

TYPE OF TEST: Ice Pack w/.008" Paper each SIDE
TEST ENGINEER:
NAME OF RIG: W/ AGITATION
PROJECT & ENG. ORDER NO.:

SHEET 1 OF 2 DATE 8-19-76
TEST PLAN NO.:
MODEL NO.:
PART NO.:
SERIAL NO.:
OPERATORS:

Time	Test Time	Volts	Current		Power	Flo Syst	Syst	Hx	Hx	Hx IN	Hx OUT	Flow Hx	Hx IN (27)	Hx OUT (28)	ΔT	LCG IN (1)	LCG OUT (2)	Wall Temp		Bad Press		Chamb Press
		AC	AMPS			GPM	%	%	%	%	Psia	GPM	°F	°F	MV	°F	°F	°F		PSIG		u
													72	72		72	72					
0920		76	1.9	3.9			82.5		150				73	65		76	79					2
0925	start						82.5		15.0				79	49	.885	74	80			5		
0930	5	76	2.0	3.8			82.5		15.0				80	41	.820	72	78					
0935	10	76	2.0	3.8			82.5		16.0				77.5	43	.755	71	77					
0940	15	76	2.0	3.8			82.5		35				76	44.0	.585	67	73					
0945	20	76	2.0	3.8			82.5		30				72	46	.585	65.5	71.5					
0950	25	76	2.0	3.8			82.5		30				71.5	45	.580	65.5	71.5					
55	30	76	2.0	3.8			82.5		20				70	40	.685	66.0	71.5					
1000	35	76	2.0	3.8			82.5		20				71.5	40.5	.670	66.5	72.5					
05	40	76	2.0	3.8			82.5		25				71.5	42.5	.640	66.0	72.0					
10	45	76	2.0	3.8			82.5		25				71.5	43	.630	66.0	72.0					
15	50	76	2.0	3.8			82.5		~~35~~ 30				72.0	47	.550	66.0	72.0					
20	55	76	2.0	3.8			82.5		35				70.5	49	.480	65.5	71.5					
25	60	76	2.0	3.8			82.5		35.0				70.5	50.5	.460	65	71.0					
30	65	76	2.0	3.8			82.5		35.0				70.5	51.0	.450	65	70.5					
35	70	76	2.0	3.8			82.5		35.0				71.0	53.0	.419	66	71.5					
40	75	76	2.0	3.8			82.5		44.0				71.5	57	.325	66	72.0					
45	80	76	2.0	3.8			82.5		69.0				72.0	62.5	.225	66	72					
50	5	76	2.0	3.8			82.5		100+				72.0	66.5	.130	67	72					
55	90	76	2.0	3.8			82.5		100+				73	68.0	.120	68	73.5					

SVHSER 7163

REMARKS:
Recheck initial temp -20°C
* changed Flowrators -

14.15 LBS KHF_2/H_2O SOLUTION

13488

HSF-175.1A 1/66

Hamilton Standard DIVISION OF UNITED AIRCRAFT CORPORATION
WINDSOR LOCKS, CONNECTICUT 06096

SPACE & LIFE SYSTEMS LABORATORY

LOG OF TEST

TYPE OF TEST: Ice Pack W/.008" Paper
TEST ENGINEER: Each SID
NAME OF RIG: W/ AGITATION
PROJECT & ENG. ORDER NO.:

SHEET: 2 of 2' DATE: 8-19-76
TEST PLAN NO.:
MODEL NO.:
PART NO.:
SERIAL NO.:
OPERATORS:

Time	Test Time	Volts	Current		Power	FC Syst	Syst	H2O	FC H2O	H2O IN	H2O OUT	FC H2O	H2O IN	H2O OUT	ΔT	LCG IN	LCG OUT	Total Tem		Bag Pres		CWS Pres
	MIN												°F	°F	MV					PSIG		
1100	95	76	1.9	3.9			82.5		100+				75.0	70.5	.105	71.0	76.0					
5	100	76	2.0	3.8			82.5		100+				77.0	73.0	.095	73.0	78.0					
10	105	76	2.0	3.8			82.5		100+				80.5	77.5	.090	75.5	80					
15	110	76	2.0	3.8			82.5		100+				82.5	79.0	.084	78.5	83.5					
20	115	76	2.0	3.8			82.5		100+				85.5	82.0	.075	80.0	85.0					

— EOT —

SVHSER 7163

REMARKS:

13489

Hamilton Standard DIVISION OF UNITED AIRCRAFT CORPORATION
WINDSOR LOCKS, CONNECTICUT 06096

SPACE & LIFE SYSTEMS LABORATORY

LOG OF TEST

TYPE OF TEST: Ice Pack KHF_2/H_2O
TEST ENGINEER: HORIZ. WICK CAVITIES
NAME OF RIG: W/PAPER BETWEEN
PROJECT & ENG. ORDER NO.

SHEET 1 OF 2 DATE 9-13-76
TEST PLAN NO.
MODEL NO.
PART NO.
SERIAL NO.
OPERATORS 1 2

Time	Test Time	Volts	Amps	Amps	Watts	Flo Syst	Syst	Hx	Hx	Hx In	Hx Out	Flow Hx	Hx In (27)	Hx Out (28)	ΔT	LCG In	LCG Out	Wall Temp		Blad Press		Chamber Press
	Min	AC				GPM	%	%	%	PSIA	PSIA	GPM	°F	°F	MN	°F	°F	°F		PSIG		
0920	0	76	1.95	3.85			82.5		14.0				71	52		71	71			7		
0925	5	76	1.95	3.85			82.5		14.75				72	36		64	70					
30	10	"	1.95	3.80			82.5		14.75				72	35.5	ΔT	64.5	70.5					
35	15	76	1.90	3.9			82.5		14.25				69.0	36.0		64.0	70.0					
40	20	76	1.90	3.9			82.5		14.0				69.5	36	Depot	64.0	70.0					
45	25	76	1.90	3.90			82.5		14.0				70.0	37		64.0	70.0					
50	30	76.	1.9	3.90			82.5		15.0				70.0	38.0	Ice	65.0	71.0					
55	35	76.0	1.95	3.85			82.5		15.0				70.0	39.0	Pack	66.0	72.0					
1000	40	76.	1.95	3.85			82.5		15.0				70	39.0		66.0	72.0					
5	45	76	1.95	3.85			82.5		15.0				69.5	40.0	Up	66.0	72.0					
10	50	76	1.95	3.85			82.5		16.0				70.5	42.0	To	66.0	72.0					
15	55	76	1.95	3.85			82.5		30*				71.0	45.5	212°	66.0	72.0					
20	60	76	1.95	3.85			82.5		35.0				70.0	48.0	deg.	66.0	72.0					
25	65	76	1.95	3.85			82.5		35.0				69.5	49.0	in	65.0	71.0					
30	70	76	1.95	3.85			82.5		35.0				69.0	50.0	Pot	64.0	70.0					
35	75	76	1.95	3.85			82.5		35.0				69.5	51.0	Pot	64	70.0					
40	80	76	1.95	3.85			82.5		38.0				70.5	54.5		66	71.0					
45	85	76	1.95	3.85			82.5		43.0				71.0	57.5	Ice	67	72.0					
50	90	76	1.95	3.85			82.5		66.0				71.5	63.0	Pack	66.0	72.5					
55	95	76	1.95	3.85			82.5		100.0				72.5	67.0		68.5	74.0					
1100	100	76	1.95	3.85			82.5		100+				74.5	69.5	End	70.0	75.0					

REMARKS:

Ice chest Temp = −20°C
* Switched Flow meters

14.15 LBS KHF_2/H_2O SOLUTION

Noll

SVHSER 7163

13443

HSF-175 1A 1/66

Hamilton Standard DIVISION OF UNITED AIRCRAFT CORPORATION
WINDSOR LOCKS, CONNECTICUT 06096

SPACE & LIFE SYSTEMS LABORATORY

LOG OF TEST

TYPE OF TEST: Ice Pack KHF_2/H_2O
TEST ENGINEER: Horie. WICK CAVITIES
NAME OF RIG: w/ PAPER BETWEEN
PROJECT & ENG. ORDER NO.

SHEET: 2 of 2 DATE 9-13-76
TEST PLAN NO.
MODEL NO.
PART NO.
SERIAL NO.
OPERATORS

Time	Test Time	Volts	Amps	Amps	Watts	Flo Syst	Syst	Hx	Hx	Hx In	Hx Out	Flow Hx	Hx In	Hx Out	ΔT	LCG In	LCG Out	Wall Temp		Blad Press		Chmb Press
1105	105	76	1.95	3.85			82.5	Full	100+				77.0	72.5		73	78					
1110	110	76	1.95	3.85			82.5	Full	100+				79.0	75.0	Δ	75	81					
15	120	〃	1.95	3.85			82.5	Full	100+				82	79.0	T	78	83					
20	125	〃	1.95	3.85			82.5	Full	100+				85.5	80.5		80	85					

ΔT NOT REQUIRED

SVHSER 7263

REMARKS:

13559

Noll